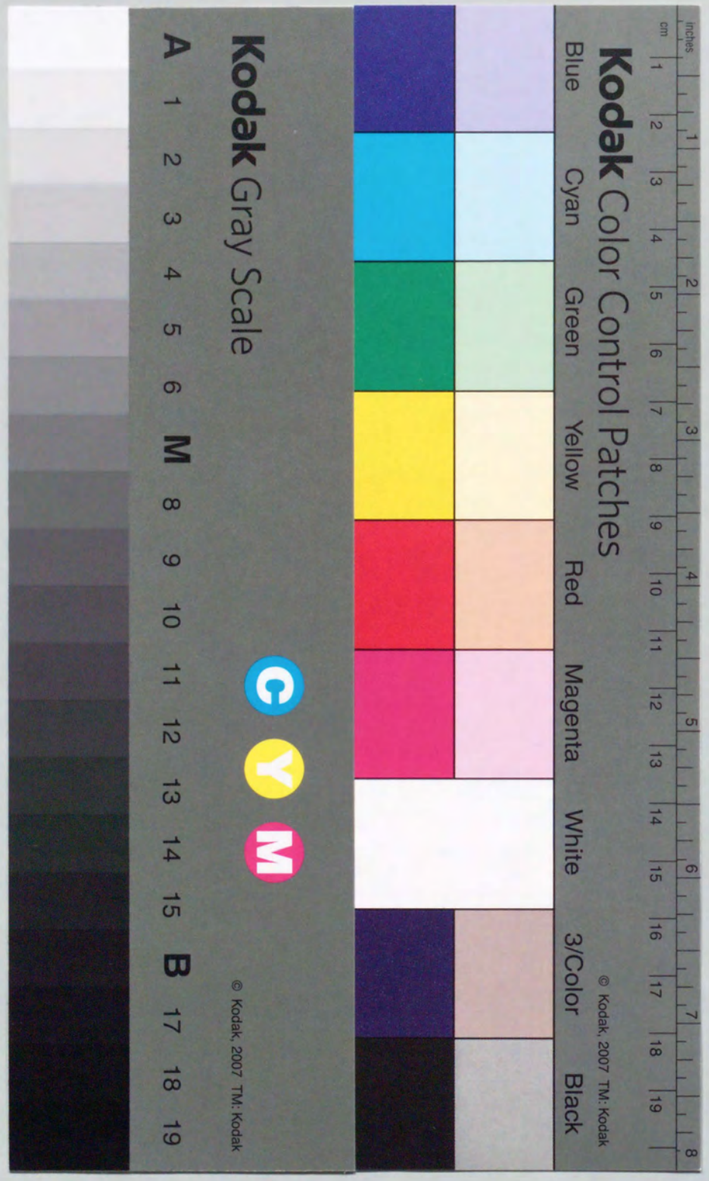

Studies on the activity and stability of ribonuclease HI from *Thermus thermophilus* HB8

(*Thermus thermophilus* HB8 由来リボヌクレアーゼ HI の

活性と安定性に関する研究)

Nobutaka Hirano

平野　展孝

2001

Department of Material and Life Science
Graduate School of Engineering
Osaka University

Studies on the activity and stability of ribonuclease HI from *Thermus thermophilus* HB8

(*Thermus thermophilus* HB8 由来リボヌクレアーゼ HI の

活性と安定性に関する研究)

Nobutaka Hirano

平野　展孝

2001

Department of Material and Life Science
Graduate School of Engineering
Osaka University

Contents

General Introduction

Understanding the stability-activity-structure relationships of proteins are expected to provide valuable information, which facilitate the understanding for the molecular basis of protein stability and enzymatic activity. This molecular basis of proteins will establish a general strategy to evolve enzymes so that they exhibit desirable thermal stability and enzymatic activity. These improved enzymes can meet the industrial expectations and develop new techniques and materials useful in various fields, such as medicine and chemical industry. For this purpose, it is believed to be a promising strategy to focus on a given pair of thermophilic and mesophilic proteins and to elucidate the mechanisms by which these two proteins exhibit different stabilities and activities. To understand the stability-activity-structure relationships of thermophilic enzymes at the atomic levels, crystal structures of a number of the thermophilic enzymes have been determined by X-ray analyses and compared with those of their mesophilic counterparts. Since the active-site structures of the thermophilic and mesophilic enzymes and most of their physicochemical characteristics are shown to be similar, the thermophilic and mesophilic enzymes are generally assumed to share the common catalytic mechanism.

Thermophilic enzymes are generally more stable but less active than their mesophilic counterparts at moderate temperatures, despite the strong resemblance in their structures and functions (1-3). Comparative studies on hydrogen/deuterium exchange of thermophilic and mesophilic enzymes (4), as well as those on dynamic motion (5), have suggested that reduction in the conformational flexibility is responsible for the highly thermal stability and poor enzymatic activity at moderate temperatures of thermophilic enzymes. In addition, introductions of a series of the amino acid substitutions around the active site of barnase (6), T4 lysozyme (7), and thermolysin (8) have also shown that the protein stability increased in proportion to the decrease in the enzymatic activity. This may lead to the suggestion that enzymes can not acquire both highly enzymatic activity at moderate temperatures and highly thermal stability.

However, this suggestion has not always been supported experimentally. For example, site-directed mutagenesis studies have demonstrated that the thermal stabilities of mesophilic enzymes can be increased significantly without cost of their enzymatic activities at moderate temperatures (9-12). Recently, in vitro evolution studies have also shown that the activity and stability of enzymes are not correlated with each other (13-17). More information on the stability-activity-structure relationships of enzymes is required to establish a method to improve the activity or stability of an enzyme.

Ribonuclease H (RNase H) is an enzyme that specifically hydrolyzes RNA strand of RNA/DNA hybrid (18), and is thought to be involved in synthesis and removal of RNA primers which are required for DNA replication, and in elimination of RNAs which are misincorporated into DNA strands. The enzyme has been used as a tool for recombinant DNA technology. For example, it is used to synthesize cDNA, because it efficiently degrades and removes mRNA that is used as a template for the synthesis of cDNA. In addition, RNase H is used for removal of polyA-tail and editing of RNA. An artificial RNA restriction enzyme by covalently attaching DNA oligomers to *E. coli* RNase HI was constructed previously, and it cleaved RNA in a sequence-specific manner (19).

RNase HI from extreme thermophile *Thermus thermophilus* HB8 (*T. thermophilus* RNase HI) and *E. coli* RNase HI have been used as a pair of thermophilic and mesophilic proteins to elucidate the mechanisms by which thermophilic enzymes acquire unusual thermostability (9-12). *T. thermophilus* and *E. coli* RNases HI are composed of 166 and 155 amino acid residues, respectively, and both act as a monomer (1, 20). According to the classification proposed by Ohtani *et al.* (21), in which RNases H are classified into two major families (Type 1 and Type 2 RNases H), these enzymes are members of the Type 1 RNase H family. Of various RNases H, *E. coli* RNase HI, which shows the amino acid sequence identity of 52% to *T. thermophilus* RNase HI, has been most extensively studied for structures and functions (22-24). *T. thermophilus* and *E. coli* RNases HI are an ideal thermophilic/mesophilic protein pair to

analyze the stabilization mechanisms of proteins, because the crystal structures of these enzymes are available (25-28) and their conformational stabilities can be analyzed thermodynamically (1, 9, 29). The three-dimensional structure of *T. thermophilus* RNase HI (28) highly resembled to that of *E. coli* RNase HI (25-27) (Fig. 1). In addition, all of the amino acid residues involved in the active-site and substrate-binding site are conserved and positioned similarly in these two structures, suggesting that *T. thermophilus* RNase HI is indistinguishable from *E. coli* RNase HI in the enzymatic functions (Fig. 2, 3), except for protein stability. The former is more stable than the latter by 33.9 °C in T_m at pH 5.5 in the presence of 1.2 M GdnHCl, and by 11.8 kcal/mol in ΔG at 25 °C and 14.1 kcal/mol in ΔG at 50 °C (1). However, only *E. coli* RNase HI has so far been mutated to identify the amino acid substitutions that make *T. thermophilus* RNase HI more stable than *E. coli* RNase HI. Therefore, I decided to make mutational studies of *T. thermophilus* RNase HI to elucidate the stability-activity-structure relationships of *T. thermophilus* RNase HI. Because high tolerance to thermal denaturation often makes thermophilic enzymes useful for industrial purposes, these studies may also allow us to develop a novel method to apply *T. thermophilus* RNase HI for industrial purposes.

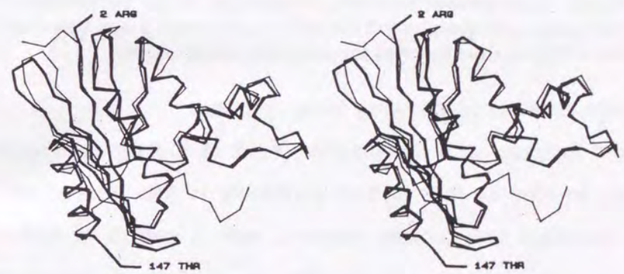

Fig. 1. Stereo view of the crystal structure of *T. thermophilus* RNase HI (thick lines) superimposed onto that of *E. coli* RNase HI (thin lines).
All of the α-carbons for *E. coli* RNase HI and the α-carbons from Arg^2 to Thr^{147} for *T. thermophilus* RNase HI are shown.

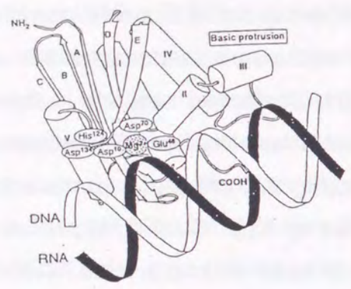

Fig. 2. Schematic representation of the model for the complex between *E. coli* RNase HI and RNA/DNA hybrid.
The positions of amino acid residues that are involved in the catalytic reaction or in the binding with the catalytically-essential Mg^{2+} ion are shown. The basic protrusion region is also indicated. For the secondary structure of an RNA/DNA hybrid, which assumes an intermediate, heteromerous duplex structure, between A-form and B-form structures, the DNA portion is shown as an open strand and the RNA portion as a solid strand.

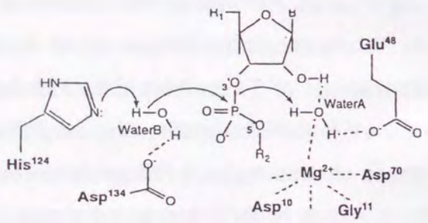

Fig. 3. A proposed catalytic mechanism of *E. coli* RNase HI.
Involvements of amino acid residues and the Mg^{2+} ion in a general acid-base mechanism for the hydrolysis of the P-O3' bond of the RNA are presented schematically.

This thesis consists of following three chapters.

Chapter 1 focuses on a stabilization factor of *T. thermophilus* RNase HI. In this chapter, to identify factors that contribute to the thermal stability of this protein, I construct the protein variants with a series of carboxyl-terminal truncations and Cys → Ala mutations. The results indicate that the formation of a disulfide bond between Cys^{41} and Cys^{149} contributes to the protein stability by 6-7 °C in T_m. This disulfide bond is not formed in vivo, but is spontaneously formed in vitro during the purification process in the absence of a reducing reagent. Therefore, the difference in the in vivo stability between *T. thermophilus* and *E. coli* RNases HI must be ~25 °C in T_m.

Chapter 2 focuses on a stability-activity relationship of this enzyme. In this chapter, I succeed in identifying three single amino acid substitutions, Ala^{12}→Ser, Lys^{75}→Met, and Ala^{77}→Pro, that increase the catalytic efficiency (k_{cat}/K_m) of *T. thermophilus* RNase HI with in vitro evolution study. Combinations of these mutations show 40-fold increase in the catalytic efficiency of this enzyme without seriously affecting its thermal stability. Therefore, these results indicate that the activity of an enzyme from extreme thermophile is not always inversely correlated with its stability.

Chapter 3 focuses on an application of this enzyme. In this chapter, I construct a DNA-linked RNase H using *T. thermophilus* RNase HI (DNA-linked TRNH), which cleaves RNA site-specifically at high temperatures. This DNA-linked TRNH cleaves the 15-mer RNA more effectively than the DNA-linked RNase H using *E. coli* RNase HI at the temperatures higher than 50 °C. Therefore, DNA-linked TRNH may be useful for the cleavage of RNA molecules with highly ordered structures at high temperatures, at which such structures of RNA molecules will be thermally denatured.

Chapter 1. A Stabilization Factor of *T. thermophilus* RNase HI

Stabilization of Ribonuclease HI from *Thermus thermophilus* HB8 by the Spontaneous Formation of an Intramolecular Disulfide Bond

1.1 Introduction

RNases HI from *Thermus thermophilus* HB8 and *E. coli* have been used as a thermophilic/mesophilic protein pair for analyses of the stabilization mechanisms of proteins. By replacing amino acid residues of *E. coli* RNase HI with those from *T. thermophilus* RNase HI (9-11) or by introducing random mutagenesis into the *E. coli* RNase HI sequence (30), four amino acid substitutions that may contribute to the higher stability of *T. thermophilus* RNase HI as compared to that of *E. coli* RNase HI have been identified. They are $Gly^{23} \rightarrow$ Ala, $His^{62} \rightarrow$ Pro, $Val^{74} \rightarrow$ Leu, and $Lys^{95} \rightarrow$ Gly, which increase the stability of *E. coli* RNase HI by 1.8, 4.1, 3.3 and 6.8 °C in T_m, respectively, at pH 5.5 in the presence of 1.0 M GdnHCl. Crystallographic (11,31) and theoretical (32, 33) studies for the *E. coli* RNase HI variants with either one of these mutations, except for that with the $Gly^{23} \rightarrow$ Ala mutation, allowed us to propose that the introduction of the proline residue into the turn region ($His^{62} \rightarrow$ Pro), the cavity-filling mutation ($Val^{74} \rightarrow$ Leu), and the replacement of the left-handed helical residue with Gly ($Lys^{95} \rightarrow$ Gly) are effective to increase the protein stability. In addition, the thermostabilizing effects of the five mutations, including these four mutations, were shown to be additive (12). However, the combination of the four stabilizing mutations can increase the stability of *E. coli* RNase HI by at most only 16.0 °C, which is less than the half of the difference between the T_m values of *T. thermophilus* and *E. coli* RNases HI. Additional stabilizing factors, which have yet to be unidentified, must contribute to the stability of *T. thermophilus* RNase HI.

The strategy to identify the factors that make *T. thermophilus* RNase HI more stable than *E. coli* RNase HI so far employed, is to introduce amino acid substitutions into *E. coli* RNase HI and look for thermostabilizing mutants. Any mutant *T. thermophilus* RNase HI protein has not been constructed for this purpose. However, because stabilizing forces or interactions are often generated from the multiple interactions, they are not always created by introducing a single amino acid substitution into *E. coli* RNase HI. On the other hand, it may be relatively easier to impair such forces or interactions by introducing a single amino acid substitution into *T. thermophilus* RNase HI. The accumulation of this information will be helpful to identify these stabilizing forces or interactions. In addition, mutational studies of *T. thermophilus* RNase HI may provide an answer to the question as to whether the difference in the in vitro stability between *T. thermophilus* and *E. coli* RNases HI reflects the difference in the in vivo stability between them, because protein stability is often affected by modifications in vitro, such as a disulfide bond formation.

Proteins from thermophilic sources usually have less cysteine residues than do the mesophilic counterparts (34). However, *T. thermophilus* RNase HI, which contains four cysteine residues, has one more cysteine residue than does *E. coli* RNase HI (Fig. 1-1). Therefore, there is a chance that the formation of a disulfide bond contributes to enhance the T_m value of this protein. It has been shown that all three cysteine residues in *E. coli* RNase HI exist in free forms and the mutations of these residues to Ala do not seriously affect the enzymatic activity (35). Two of the four cysteine residues (Cys^{13} and Cys^{63}) in *T. thermophilus* RNase HI are conserved in the sequences of these enzymes. Cys^{13} is located at the βA strand and is relatively buried inside the protein molecule. Cys^{63} is located at the loop between the αI helix and the βD strand and is exposed to the solvent. The other two cysteine residues (Cys^{41} and Cys^{149}) are located at the turn between the βC strand and the αI helix, and at the C-terminal region, respectively. Since *T. thermophilus* RNase HI is present in a reducing environment, all of the cysteine residues must exist in reduced forms in vivo. Structural and biochemical characterizations of the recombinant protein

purified from *E. coli* suggested that they exist in reduced forms in vitro as well (1, 28). Namely, the backbone structure of the protein, which is available for the residues from Arg^{2} to Thr^{147}, clearly shows that Cys^{13} and Cys^{63} exist in reduced forms. In addition, because structural disorder of the carboxyl-terminal (C-terminal) 14 amino acid residues, including Cys^{149}, in the electron density map (28), it is unlikely that a disulfide bond is fully formed between Cys^{41} and Cys^{149}. Chemical modification with 5,5'-dithiobis-(2-nitrobenzoic acid) (DTNB) has also suggested that all of the cysteine residues exist in reduced forms (1). However, these results cannot rule out the possibility that a disulfide bond is formed between Cys^{41} and Cys^{149} at a different conditions, especially those in which thermal denaturation of the protein is examined.

In the C-terminal region of *T. thermophilus* RNase HI, four proline residues are clustered at the positions of 148, 150, 151, and 154, whereas, no proline residues are located at the corresponding region of *E. coli* RNase HI. It has been reported that the thermophilic proteins have more proline residues than mesophilic proteins (36). In fact, proline residues have been shown to contribute to increasing protein stability when they are located at the β-sheet or the turn/loop region, because the entropy of the unfolded state of the protein is decreased (37). Therefore, I have decided to introduce a series of the truncations into the C-terminal region of *T. thermophilus* RNase HI, to analyze the role of the proline and cysteine residues located in this region on the protein stability.

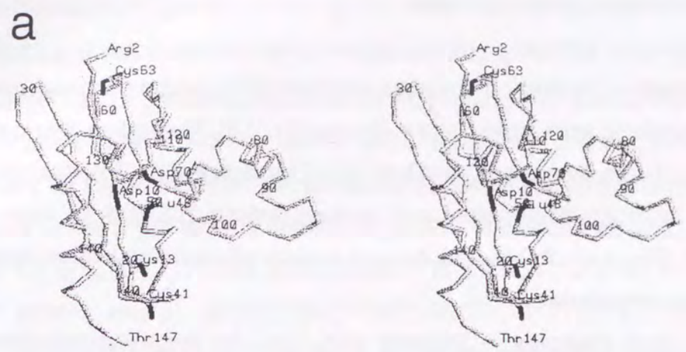

Fig. 1-1. Structure of *T. thermophilus* RNase HI.

(a) This stereo view of the backbone structure of *T. thermophilus* RNase HI, determined by Ishikawa *et al.* (28), was drawn with the program RasMol. *Numbers* represent the positions of the amino acid residues, which start from -4 for the initiator methionine of the protein. The initiator methionine starts at -4, because the *T. thermophilus* RNase HI sequence contains an additional four residues at the N-terminus as compared to the *E. coli* RNase HI sequence (1). Arg^{2} and Thr^{147} represent the N and C-terminal residues in this crystal structure. The side chains of Cys^{13}, Cys^{41}, and Cys^{63} are indicated by solid lines. The Cα atoms of the active site residues (Asp^{10}, Glu^{48}, and Asp^{70}) are also indicated by solid lines. This crystal structure of *T. thermophilus* RNase HI has been deposited in the Protein Data Bank, with the accession number 1RIL. (b) The amino acid sequence of *T. thermophilus* RNase HI, determined by Kanaya and Itaya (1), is shown. The ranges of the five α-helices and the five β-strands are shown along the sequence. All four cysteine residues, at positions 13, 41, 63, and 149, are shown in ***boldface***, and the three catalytically essential carboxylates (Asp^{10}, Glu^{48}, and Asp^{70}) are underlined. The N-terminal region from Met^{-4} to Pro^{1} and the C-terminal region from Pro^{148} to Ala^{161}, which have not been defined by crystallographic analyses, probably due to structural disorder, are boxed.

1. 2 Experimental Procedures

Materials — Restriction enzymes and modifying enzymes for recombinant DNA technology were from Takara Shuzo Co., Ltd. Guanidine hydrochloride (GdnHCl) of ultra pure grade was from ICN Biomedicals Inc. Phosphocellulose (P-11) was from Whatman. Lysyl endopeptidase (LEP) was from Wako Chemical Co., Ltd. Acetylated bovine serum albumin was from Bethesda Research Laboratories.

Cells and Plasmids — Plasmid pJAL700T for the overproduction of *T. thermophilus* RNase HI was constructed previously (1). This plasmid bears the wild-type *rnhA* gene under the control of the bacteriophage λ promoters P_R and P_L, the cI^{ts857} gene, and the bacteriophage fd transcription terminator. Competent cells of *E. coli* HB101 (F-, *hsd S20, recA13, ara-14, proA2, lac Y1, gal K2, rps L20(str), xyl-5, mtl-1, sup E44, leuB6, thi-1*) were from Takara Shuzo Co., Ltd.

Mutagenesis — The mutant *rnhA* genes, encoding the *T. thermophilus* RNase HI variants with a series of the C-terminal truncations, were constructed by PCR using a 5' primer with an *Nde*I site and 3' mutagenic primers with *Sal*I sites. The sequence of the 5' primer was 5'-GCGAATTCCAT*ATG*AATCCATCACCTAGAAAA-3', where the initiation codon of the *rnh* gene is shown in *italic* type and the underlined bases show the position of the *Nde*I site. The 3' mutagenic primers were designed to replace the codon for the amino acid residue 144, 146, 148, 149, 150, 152, 154, or 156 with the TAA termination codon. Their sequences were 5'-GCGTCGAC*TTA*-$(B)_n$-3', where the sequence complementary to the termination codon of the *rnh* gene is shown in *italic* type, and the underlined bases show the position of the *Sal*I site. $(B)_n$ represents the 18-19 bases with the sequences that are complementary to the 3'-terminal region of the *rnhA* gene. The truncated proteins are designated as TRNH[ΔX], where X represents the truncated at the C-terminus. For example, TRNH[Δ150-161] represents the truncated protein lacking the C-terminal 12 residues from positions 150 to 161.

The mutant *rnhA* genes, encoding the mutant proteins, in which single or multiple Cys → Ala mutations were introduced into either the wild-type protein or TRNH[Δ150-161], were constructed by PCR using a 5' primer with an *Nde*I site, a 3' primer with a *Sal*I site, and 5' and 3' mutagenic primers, as described previously for the construction of the mutant *E. coli* RNase HI proteins (38). The sequence of the 5' primer was mentioned above. The sequence of the 3' primer were 5'-GCGTCGACCTTAAAGGTGGGGCTTTCCCGGTCC-3' for the full-size mutant protein and 5'- GCGTCGACTTAGCAGGGCGTTTTGGCCTGGGAC-3' for the TRNH[Δ150-161] mutant proteins, where the underlined bases show the positions of the *Sal*I sites. The mutagenic primers were designed so that the codons for Cys^{13} and Cys^{41} were changed from TGC to GCC for Ala, and the codon for Cys^{63} was changed from TGC to GCA for Ala. Since the 3' primer includes the sequence complementary to the codon for Cys^{149}, the TGC codon for Cys^{149} was changed to GCC, for the construction of the TRNH[Δ150-161] derivatives, in which Cys^{149} is replaced by Ala. The mutant *rnhA* genes, encoding the TRNH[Δ150-161] variants with a series of substitutions at the C-terminus (Cys^{149}), were constructed by PCR using the 5' primer mentioned above and the 3' mutagenic primers with the sequences of 5'-GCGTCGACTTANNNGGGCGTTTTGGCCTGGGAC-3', where the underlined bases show the position of the *Sal*I site and NNN represents the sequence complementary to the codon for the mutated residue. The 3' mutagenic primers were designed so that the TGC codon for Cys^{149} was changed to TCC for Ser, ACC for Thr, GTC for Val, and ATC for Ile. The resultant derivatives of the wild-type protein and TRNH[Δ150-161] are designated as X'-TRNH and X'-TRNH[Δ150-161], respectively, in which X' represent(s) the amino acid residue(s) at position(s) 13, 41, 63, and/or 149 (one-letter notation). For example, A^{149}-RNase HI represents the mutant protein in which Cys^{149} of the wild-type protein is replaced by Ala, and $A^{13}A^{63}$-TRNH[Δ150-161] represents the mutant protein in which Cys^{13} and Cys^{63} of TRNH[Δ150-161] are replaced by Ala.

All primers were synthesized by Sawady Technology Co., Ltd. PCR was

performed for 25 cycles with Perkin Elmer GeneAmp PCR System 2400, using Vent DNA polymerase from New England Biolabs, Inc. All of the nucleotide sequences of the mutant *rnh* genes were confirmed by the dideoxy chain termination method (39). After digestion by *Nde*I and *Sal*I, the PCR fragments were ligated into the *Nde*I-*Sal*I sites of the plasmid pJAL700T to construct the expression vectors for the mutant proteins. The overproducing strains were constructed by transforming *E. coli* HB101 with the resultant expression vectors.

Overproduction and Purification — Cultivation of the *E. coli* HB101 transformants with the plasmid pJAL700T derivatives, overproduction of the truncated and mutant proteins, and preparations of the crude extracts (lysates) from cells were carried out as described previously for those of the wild-type protein (1). However, the following purification procedures were slightly modified, as described below. For the purification of the wild-type, truncated, and mutant proteins, except for TRNH[Δ148-161], ammonium sulfate was added to the crude lysates to the concentration of 80%, and the resultant precipitates were collected by the centrifugation at 15,000 x *g* for 30 min at 4 °C. They were then suspended in 40 ml of 10 mM Tris-HCl (pH 7.5) containing 1 mM EDTA (TE buffer), dialyzed against the TE buffer using a Dialysis Membrane (Size 20) from Viskase Sales Corporation, and applied to a column (3 ml) of P-11 equilibrated with the TE buffer. After washing the column with the TE buffer, the enzyme was eluted from the column with a linear gradient of NaCl from 0 to 0.5 M in the TE buffer. The protein fractions eluted at an NaCl concentration of approximately 0.3 M were pooled. For the purification of TRNH[Δ148-161], 1 M sodium acetate (pH 5.5) was added to the crude lysate to the concentration of 20 mM. This solution was applied to a column (3 ml) of P-11 equilibrated with 20 mM sodium acetate (pH 5.5) containing 0.2 M NaCl. After washing the column with 20 mM sodium acetate (pH 5.5) containing 0.2 M NaCl, the enzyme was eluted from the column with a linear gradient of NaCl from 0.2 to 1 M in 20 mM sodium acetate (pH 5.5). The protein fractions eluted at an NaCl concentration of approximately 0.7 M were pooled.

The protein concentration was determined from UV absorption, assuming that the mutant proteins obtained in this experiment have the same $A_{280}^{0.1\%}$ value of 1.6 as that of the wild-type protein (1). The cellular production levels of the mutant (truncated) proteins and their purities were estimated by subjecting whole cell lysates to SDS-PAGE on a 15 % polyacrylamide gel (40), followed by staining with Coomassie Brilliant Blue. The molecular weight of each truncated protein was estimated by applying an aliquot of the purified sample to a column (1.6 x 100 cm) of Sephacryl S-300 (Pharmacia) equilibrated with 10 mM Tris-HCl (pH 7.5) containing 0.1 M NaCl. The fractions of 2.5 ml were collected. The flow rate was 10 ml/h. Bovine serum albumin (67K), ovalbumin (43K), chymotrypsinogen A (25K), and RNase A (13.7 K) were also applied individually to the column as standard proteins.

RNase H Activity — The enzymatic activity was basically determined in 10 mM Tris-HCl (pH 8.0) containing 10 mM $MgCl_2$, 50 mM NaCl, 1 mM 2-mercaptoethanol (2-Me), and 100 μg/ml bovine serum albumin at 30 °C by measuring the radioactivity of the acid-soluble digestion product from a ^{3}H-labeled M13 RNA/DNA hybrid, as described previously (29). The concentration of 2-Me was changed to 0 or 100 mM, when the effect of 2-Me on the enzymatic activity was analyzed.

Circular Dichroism Spectra — The CD spectra were measured on a J-720W automatic spectropolarimeter from Japan Spectroscopic Co., Ltd. at 10 ℃ in 10 mM Tris-HCl (pH 7.5) containing 1 mM EDTA. For the measurement of the far-ultraviolet (UV) CD spectra (200-260 nm), the protein concentration was approximately 0.13 mg/ml, and a cell with an optical path length of 2 mm was used. For the measurement of the near-UV CD spectra (250-320 nm), the protein concentration was 0.5 - 1.0 mg/ml and a cell with an optical path length of 10 mm was used. The mean residue ellipticity, θ, which has the units of deg cm^2 $dmol^{-1}$, was calculated by using an average amino acid molecular weight of 110.

Thermal Denaturation — The thermal denaturation curves and the

temperature of the midpoint of the transition, T_m, were determined as described previously (9) by monitoring the change in the CD value at 220 nm. The proteins were dissolved in 20 mM sodium acetate (pH 5.5) containing 1 M guanidine hydrochloride (GdnHCl), unless specifically described. The protein concentration was approximately 0.13 mg/ml and a cell with an optical path length of 2 mm was used. The enthalpy change of unfolding at the T_m (ΔH_m) and the entropy change of unfolding at the T_m (ΔS_m) were calculated by van't Hoff analysis. The difference in the free energy change of unfolding between the mutant and wild-type proteins, at the T_m of the wild-type protein ($\Delta\Delta G_m$), was estimated by the relationship given by Becktel and Schellman (41), $\Delta\Delta G_m = \Delta T_m \cdot \Delta S_m$ (wild-type protein). ΔT_m is the change in T_m of a mutant protein relative to that of the wild-type protein. Becktel and Schellman pointed out that it was possible to relate the ΔT_m to $\Delta\Delta G_m$. This is demonstrated in Fig 1-2. The slanting lines are the curves for ΔG of the wild-type and the mutant proteins. These lines cross the abscissa at their T_m. The $\Delta\Delta G_m$ is a vertical line connecting the two curves at T_m of the wild-type and the mutant proteins. Since $\partial\Delta G/\partial T = -\Delta S$, the slopes of the two curves at their T_m are their $-\Delta S_m$. If the stability curve of the mutant protein can be approximated as a straight line, slope = $\Delta\Delta G_m/\Delta T_m$ or $\Delta\Delta G_m = \Delta T_m \cdot \Delta S_m$ (mutant protein). If the stability curves can be assumed as a parallel, the ΔS_m for the mutant protein can be approximated by the ΔS_m for the wild-type protein, $\Delta\Delta G_m = \Delta T_m \cdot \Delta S_m$ (wild-type protein). Generally, the error in the ΔS_m value is greater than the error in the T_m value. Moreover, the ΔS_m value for the wild-type protein is generally known with greater certainty than the ΔS_m value for the mutant protein. Therefore, I estimated $\Delta\Delta G_m$ values for all of the mutant proteins by using $\Delta\Delta G_m = \Delta T_m \cdot \Delta S_m$ (wild-type protein). The ΔS_m value of the wild-type protein was determined to be 0.437 kcal/(mol·K) from four independent experiments with errors of ±0.04 kcal/(mol·K). This value was used

for the calculation of the $\Delta\Delta G_m$ values. The theoretical curves for unfolding were drawn on the assumption that the protein unfolds by a two-state mechanism, using the experimentally determined T_m and ΔH_m values, and the ΔCp value of 1.79 kcal/mol determined for *E. coli* RNase HI (42).

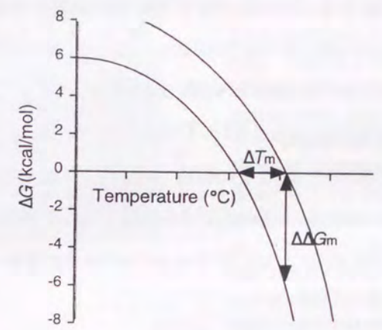

Fig. 1-2. The relationship between changes in melting temperature and changes in free energy. An explanation of the terms in this figure is given in the text.

Peptide-mapping analysis — Proteins were digested in 0.1 M Tris-HCl (pH 9.0) at 37 °C for 1 h with lysyl endopeptidase (LEP) at an enzyme/substrate ratio of 1:50. The resultant peptides were separated by reverse-phase HPLC on a Cosmosil ODS column (4.6 mm x 150 mm) from NACALAI tesque using a HPLC apparatus from Shimadzu LC-10A. The molecular weight of each peptide was analyzed by an on-line mass spectrometry equipment LCQ from Finnigan MAT, using electrospray ionization.

1. 3 Results

C-Terminal Truncations Design — The backbone structure of *T. thermophilus* RNase HI, which has been determined for the residues from Arg^{2} to Thr^{147} with a 2.8 Å resolution (28), as well as the amino acid sequence of the protein, are shown in Fig.1-1. Since my initial purpose was to understand the role of the C-terminal residues in the protein stability and the enzymatic activity, I decided to construct mutant proteins with a series of the C-terminal truncations. The mutant proteins TRNH[Δ148-161]~TRNH[Δ156-161] were constructed to analyze the roles of cysteine and proline residues located at the C-terminal region. The mutant proteins TRNH[Δ144-161] and TRNH[Δ146-161] were constructed to analyze the tolerance of the enzyme for the additional C-terminal truncations.

Purifications of Truncated proteins — All of the truncated proteins that were overproduced in *E. coli* HB101, were recovered in a soluble form after sonication lysis, although the more truncated forms showed a tendency to accumulate in an insoluble form (Fig. 1-3). It has previously been shown that the wild-type protein in the crude lysate obtained after sonication lysis binds to P-11 at pH 5.5 in the presence of 8 M urea but does not bind to it in the absence of 8 M urea (1). Since C-terminal truncations may alter a property of the protein, I have examined whether the truncated proteins bind to P-11 in the absence of 8 M urea. Consequently, I found that only TRNH[Δ148-161] bound to P-11 in the absence of 8 M urea. In addition, I found that the wild-type and all of the other truncated proteins bound to it if they had been precipitated by the addition of ammonium sulfate beforehand. The reason TRNH[Δ148-161] effectively bound to P-11, in the absence of 8 M urea and without the ammonium sulfate precipitation, remains to be determined. The purification yields were roughly 25 % for the wild-type and all of the truncated proteins. The amounts of the proteins purified from 1-L culture, which gradually decreased as the size of the truncated region increased and ranged from 11 to 22 mg for these proteins. Gel

filtration with Sephacryl S-300 indicated that all of the truncated proteins existed in a monomeric form, like the wild-type protein.

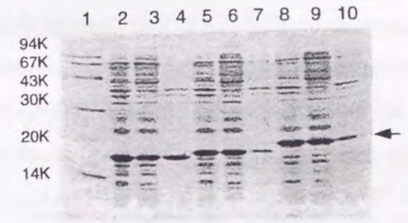

Fig. 1-3. Productions of truncated proteins in cells.
The production levels of the *T. thermophilus* RNase HI variants with the C-terminal truncations in cells were analyzed by 15 % SDS-PAGE for the wild-type protein (lanes 8-10), TRNH[Δ149-161] (lanes 5-7), and TRNH[Δ144-161] (lanes 2-4). The gel was stained with Coomassie Brilliant Blue. Lanes 2, 5, 8: whole cell extract; lanes 3, 6, 9: soluble fraction obtained after sonication lysis; and lanes 4, 7, 10: insoluble fraction obtained after sonication lysis. Size marker proteins in lane 1 are phosphorylase b for 94K, bovine serum albumin for 67K, ovalbumin for 43K, carbonic anhydrase for 30K, trypsin inhibitor for 20K, and α-lactalbumin for 14K.

Stability and Activity of Truncated Proteins — To analyze the effects of the C-terminal truncations on the protein stability, the thermal denaturation curves were measured by monitoring the change in the CD values at 220 nm (Fig. 1-4).

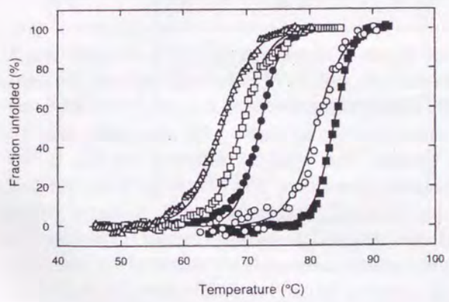

Fig. 1-4. Thermal denaturation curves of the wild-type and truncated proteins.
The apparent fraction of unfolded protein is shown as a function of temperature. Thermal denaturation curves of all proteins were determined at pH 5.5 in the presence of 1 M GdnHCl by monitoring the change in the CD value at 220 nm, as described under "Experimental Procedures". The curves of the wild-type (■), TRNH[Δ150-161] (○), TRNH[Δ149-161] (●), TRNH[Δ146-161] (□), and TRNH[Δ144-161] (△) proteins are shown as representatives. The theoretical curves for unfolding were drawn as described in Experimental Procedures.

Since the truncated proteins of *T. thermophilus* RNase HI were constructed to identify factors that make it more stable than *E. coli* RNase HI, and the

stabilities of a variety of the thermostabilizing mutants of *E. coli* RNase HI have been analyzed in the presence of 1 M GdnHCl at pH 5.5, the stabilities of the *T. thermophilus* RNase HI mutants were analyzed under these conditions. The enzyme was shown to reversibly unfold in a single cooperative fashion at these conditions with the T_m value of 83.7 °C. This value was 1.6 °C higher than that previously reported, because the thermal denaturation curve of the enzyme was previously measured at pH 5.5 in the presence of 1.2 M GdnHCl, instead of 1 M GdnHCl (1). The thermodynamic parameters of the truncated proteins, as well as their enzymatic activities relative to that of the wild-type protein, are summarized in Table 1-1.

Table 1-1
Enzymatic activities and thermodynamic parameters of mutant proteins with C-terminal truncations

Protein	Relative Activity (%)	T_m (°C)	ΔT_m (°C)	ΔH_m (kcal/mol)	$\Delta\Delta G_m$ (kcal/mol)
WT-TRNH	100	83.7		155	
TRNH [Δ156-161]	100	83.3	-0.4	94	-0.2
TRNH [Δ154-161]	100	82.0	-1.7	105	-0.7
TRNH [Δ152-161]	92	80.0	-3.7	89	-1.6
TRNH [Δ150-161]	92	80.9	-2.8	109	-1.2
TRNH [Δ149-161]	74	72.0	-11.7	135	-5.1
TRNH [Δ148-161]	69	68.1	-15.6	87	-6.8
TRNH [Δ146-161]	70	69.1	-14.6	104	-6.4
TRNH [Δ144-161]	45	66.7	-17.0	86	-7.4

The enzymatic activity was determined at 30 °C for 15 min in 10 mM Tris-HCl (pH 8.0) containing 10 mM $MgCl_2$, 50 mM NaCl, 100 μg/ml bovine serum albumin, and 1 mM 2-mercaptoethanol, by using M13 RNA/DNA hybrid as a substrate. The specific activity of the wild-type protein (WT-TRNH) was ~2.0 units/mg in this condition. Relative activity was calculated by dividing the enzymatic activity of the mutant protein by that of the wild-type protein. The melting temperature, T_m, is the temperature of the midpoint of the thermal-denaturation transition. The difference in the melting temperature between the wild-type and mutant proteins (ΔT_m) is calculated as T_m(mutant protein) — T_m(WT-TRNH). ΔH_m is the enthalpy change of unfolding at T_m calculated by van't Hoff analysis. The change in the free energy of unfolding of the mutant protein relative to that of the wild-type protein ($\Delta\Delta G_m$) was estimated by the relationship given by Becktel and Schellman (41): $\Delta\Delta G_m = \Delta T_m \cdot \Delta S_m$ (WT-TRNH). The ΔS_m value of 0.437 kcal/(mol·K), which was determined from four independent experiments with errors of ± 0.04 kcal/(mol·K), was used for the calculation of the $\Delta\Delta G_m$ values. Errors are within 30 % for the enzymatic activity, ± 0.5 °C for T_m, ± 15 kcal/mol for ΔH_m, and ± 0.2 kcal/mol for $\Delta\Delta G_m$.

The truncated protein TRNH[Δ150-161] was less stable than the wild-type protein only by 2.8 °C in T_m and 1.2 kcal/mol in ΔG_m, whereas TRNH[Δ149-161] was less stable than the wild-type protein by 11.7 °C in T_m and 5.1 kcal/mol in ΔG_m. The enzymatic activities of these truncated proteins were 92 % and 74 % of that of the wild-type enzyme. These results indicated that the C-terminal truncations of up to 12 residues did not seriously affect either the protein stability or the enzymatic activity, but additional truncation of Cys^{149} considerably decreased the protein stability without seriously affecting the enzymatic activity. Since the stabilities and enzymatic activities of the truncated proteins gradually decreased as the number of the truncated residues increased beyond 13, but those of TRNH[Δ144-161] were comparable with those of TRNH[Δ149-161], further truncations of up to five residues again did not seriously affect the protein stability or the enzymatic activity. The far- and near-UV CD spectra of the truncated proteins suggested that the C-terminal truncations of up to 18 residues did not seriously influence the secondary and tertiary structures of the protein (Fig. 1-5). These results indicate that none of the four proline residues clustered in the C-terminal region contributes to either the enzymatic activity or the thermal stability of the protein, but Cys^{149} greatly contributes to the protein stability.

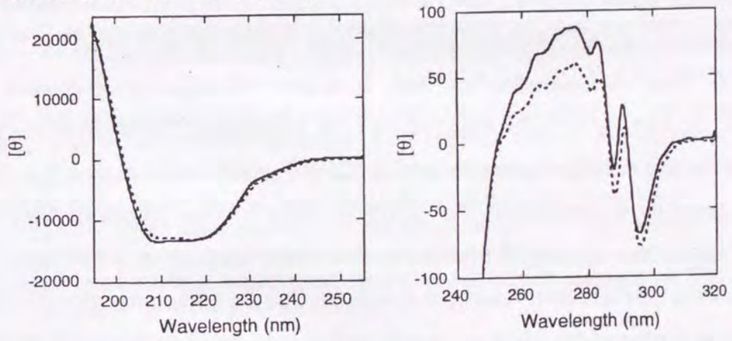

Fig. 1-5. CD spectra of the wild-type and truncated proteins.
The CD spectra of the wild-type and all truncated proteins were measured as described under "Experimental Procedures". The far-UV (left) and near-UV (right) CD spectra of the wild-type protein (solid line) and TRNH[Δ144-161] (broken line) are shown. The spectra of all other truncated proteins are slightly different from those of the wild-type protein, but with a lesser extent than are those of TRNH[Δ144-161].

Stabilities and Activities of Cys Mutants — To examine whether Cys^{149} contributes to the protein stability by forming a disulfide bond, the TRNH[Δ150-161] variants with single or multiple Cys → Ala mutations, as well as A^{149}-RNase HI, in which Cys^{149} of the wild-type protein is replaced by Ala, were constructed. If a disulfide bond involving Cys^{149} as one partner contributed to the protein stability, then the mutation of a cysteine residue that is the other partner would reduce the protein stability. The purification procedures for the Cys mutants were identical to those for the parent proteins, and the amounts of the mutant proteins purified from 1-L cultures were roughly the same as those of the parent proteins. The stabilities and activities of these Cys mutants are summarized in Table 1-2. The mutation of Cys^{41} or Cys^{149} in TRNH[Δ150-161] decreased the protein stability by 8.4-9.2 °C in T_m (3.7-4.0 kcal/mol in ΔG_m), whereas the mutation of either Cys^{13} or Cys^{63} decreased it by only 0.8-2.1 °C in T_m (0.4-0.9 kcal/mol in ΔG_m). Similar phenomena were observed for the TRNH[Δ150-161] variants with multiple Cys → Ala mutations. Namely, the double mutant protein $A^{13}A^{63}$-TRNH[Δ150-161], which contains only two cysteine residues (Cys^{41} and Cys^{149}), was less stable than TRNH[Δ150-161] by only 2.4 °C in T_m (1.1 kcal/mol in ΔG_m), whereas the Cys-free mutant protein $A^{13}A^{41}A^{63}A^{149}$-TRNH[Δ150-161] was less stable than it by 12.0 °C in T_m (5.2 kcal/mol in ΔG_m). The difference in T_m between $A^{13}A^{63}$-TRNH[Δ150-161] and $A^{13}A^{41}A^{63}A^{149}$-TRNH[Δ150-161] (9.6 °C) was comparable to that between TRNH[Δ150-161] and A^{41}-TRNH[Δ150-161] or C^{149}-TRNH[Δ150-161]. In addition, A^{149}-RNase HI was less stable than the wild-type protein by 9.0 °C in T_m (3.9 kcal/mol in ΔG_m). These results strongly suggest that the disulfide bond formed between Cys^{41} and Cys^{149} contributes equally to increasing the stabilities both of TRNH[Δ150-161] and the wild-type protein. Among the various Cys mutants, only those in which Cys^{13} was replaced by Ala had considerably less enzymatic activity than the wild-type protein, suggesting that only Cys^{13} is important for the enzymatic activity.

Table 1-2
Enzymatic activities and thermodynamic parameters of the *T. thermophilus* RNase HI and TRNH [Δ150-161] variants

Protein	Relative Activity (%)	T_m (°C)	ΔT_m (°C)	ΔH_m (kcal/mol)	$\Delta\Delta G_m$ (kcal/mol)
WT-TRNH	100	83.7		155	
WT-TRNH (reduced) [a]	100	77.4	-6.3	94	-2.8
A^{149}-TRNH	100	74.7	-9.0	117	-3.9
TRNH [Δ150-161]	100	80.9		109	
A^{13}- TRNH [Δ150-161]	17	80.1	-0.8	106	-0.4
A^{41}- TRNH [Δ150-161]	92	71.7	-9.2	143	-4.0
A^{63}- TRNH [Δ150-161]	99	78.8	-2.1	112	-0.9
A^{149}- TRNH [Δ150-161]	87	72.5	-8.4	135	-3.7
$A^{13}A^{63}$- TRNH [Δ150-161]	11	78.5	-2.4	110	-1.1
$A^{13}A^{63}$- TRNH [Δ150-161] (oxidized) [b]	9	78.5	-2.4	112	-1.1
$A^{13}A^{63}$- TRNH [Δ150-161] (reduced) [a]	11	71.6	-9.3	93	-4.1
$A^{13}A^{41}A^{63}A^{149}$- TRNH [Δ150-161]	18	68.9	-12.0	124	-5.2
S^{149}- TRNH [Δ150-161]	129	73.1	-7.8	121	-3.4
I^{149}- TRNH [Δ150-161]	115	74.6	-6.3	125	-2.8
T^{149}- TRNH [Δ150-161]	168	75.0	-5.9	126	-2.6
V^{149}- TRNH [Δ150-161]	139	75.8	-5.1	139	-2.2

The enzymatic activities and the thermal stabilities of the *T. thermophilus* RNase HI and TRNH [Δ150-161] variants were determined as described in the legend for Table 1. The relative activity of the *T. thermophilus* RNase HI variant (A^{149}-TRNH) was calculated by dividing the enzymatic activity of this mutant proteins by that of the wild-type protein. The relative activities of the TRNH [Δ150-161] variants were calculated by dividing the enzymatic activity of the mutant protein by that of TRNH [Δ150-161]. Likewise, the ΔT_m value is calculated as T_m(mutant protein) — T_m(WT-TRNH) for A^{149}-RNase HI and as T_m(mutant protein) — T_m(TRNH [Δ150-161]) for the TRNH [Δ150-161] variants. The $\Delta\Delta G_m$ value is calculated as $\Delta\Delta Gm = \Delta T_m \cdot \Delta S_m$ (WT-TRNH) for A^{149}-TRNH and as $\Delta\Delta G_m$ (mutant protein) — $\Delta\Delta G_m$ (TRNH [Δ150-161]) for the TRNH [Δ150-161] variants, in which the $\Delta\Delta G_m$ (mutant protein) and $\Delta\Delta Gm$ (TRNH [Δ150-161]) values were calculated as $\Delta\Delta G_m = \Delta T_m \cdot \Delta S_m$ (WT-TRNH). Errors are the same as those described in the legend for Table 1-1.

[a]The enzymatic activity was determined in the presence of 100 mM 2-Me and the thermal denaturation curve was measured in the presence of 20 mM 2-Me.

[b]The protein was thermally denatured and then renatured at room temperature. The enzymatic activity was determined in the absence of 2-Me.

Disulfide Bond Identification — To identify a putative disulfide bond in either the wild-type protein or TRNH[Δ150-161], peptide-mapping analyses were carried out. When these proteins were digested by lysyl endopeptidase (LEP) at pH 9.0, peptides with a variety of disulfide bonds, including Cys^{13}-Cys^{13}, Cys^{41}-Cys^{41}, Cys^{63}-Cys^{63}, and Cys^{149}-Cys^{149}, were produced (data not shown). In addition, all four kinds of the peptides with reduced cysteine residues were produced. These results indicate that the wild-type protein and the TRNH[Δ150-161] mutant protein contain a disulfide bond, but the peptide with this disulfide bond are not stable, because of the acceleration of the sulfhydryl/disulfide exchange reactions upon proteolysis. Attempts to digest the protein with LEP or other proteases at a pH lower than 7, which would suppress the sulfhydryl/disulfide exchange reactions, have thus far been unsuccessful, because the protein is not effectively cleaved under these conditions. Therefore, I decided to digest $A^{13}A^{63}$-TRNH[Δ150-161] with LEP. Since $A^{13}A^{63}$-TRNH[Δ150-161] contains only two cysteine residues at positions 41 and 149, the sulfhydryl/disulfide exchange reactions occur only when the disulfide bond is partially formed between these cysteine residues. When it was digested by LEP and the resultant peptides were analyzed by reverse-phase HPLC, the peptide with reduced Cys^{41} and the peptides with the disulfide bond between Cys^{41} and Cys^{41} and between Cys^{41} and Cys^{149} were detected (Fig. 1-6b). In this case, the peptide with reduced Cys^{149} and that with the disulfide bond between Cys^{149} and Cys^{149} should be generated by the LEP digestion, but they must elute in the flowthrough fraction of the reverse-phase column, probably because of their poor hydrophobicities. In contrast, when $A^{13}A^{63}$-TRNH[Δ150-161], which was thermally denatured and then renatured at mild temperatures, was digested by LEP, only the peptide with the disulfide bond between Cys^{41} and Cys^{149} was detected (Fig. 1-6c). These results suggest that the disulfide bond between Cys^{41} and Cys^{149} is partially (~80 %) formed in $A^{13}A^{63}$-TRNH[Δ150-161], when the protein was purified in the absence of a reducing reagent, but was fully formed once the protein was thermally denatured. When $A^{13}A^{63}$-TRNH[Δ150-161] was digested by LEP in the presence of a reducing reagent,

only the peptide with reduced Cys^{41} was detected, as expected (Fig. 1-6a). Attempt to isolate $A^{13}A^{63}$-TRNH[Δ150-161] in a reduced form have thus far been unsuccessful, because it is unstable in the absence of a reducing reagent and is gradually converted to an oxidized forms when the reducing reagent is removed. Since the enzymatic activities of the reduced and oxidized forms of $A^{13}A^{63}$-TRNH[Δ150-161], relative to that of the parent truncated protein, were similar to each other (Table 1-2), the formation of the disulfide bond between Cys^{41} and Cys^{149} did not seriously affect the enzymatic activity.

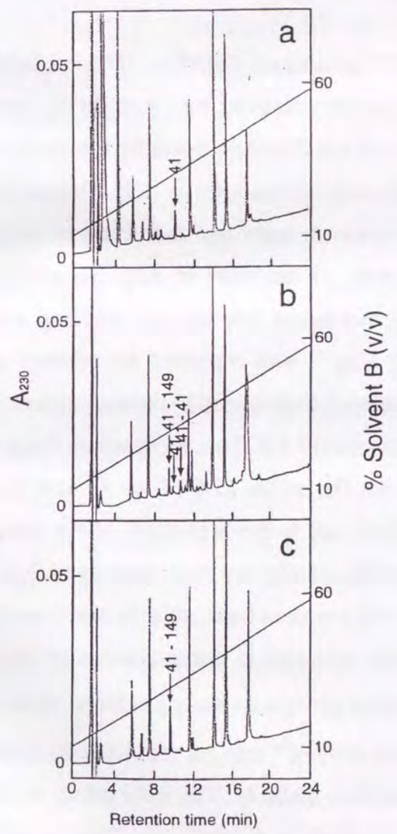

Fig. 1-6. Separation of lysyl endopeptidase digests of $A^{13}A^{63}$-TRNH[Δ150-161] in reduced and oxidized forms on reverse-phase HPLC.

The mutant protein $A^{13}A^{63}$-TRNH[Δ150-161] purified from *E. coli* was digested by lysyl endopeptidase (LEP) in the presence (a) or absence (b) of 1 mM 2-Me as described under "Experimental Procedures". Likewise, $A^{13}A^{63}$-TRNH[Δ150-161], which was thermally denatured and then renatured at room temperature, was digested by LEP (c). The resultant LEP digests (0.5 nmol) were applied on a Cosmosil ODS column (4.6 x 150 mm) equilibrated with 10 % (v/v) solvent B in solvent A. Elution was performed by raising linearly the concentration of solvent B in solvent A from 10 % to 60 % (v/v) in 25 min. Solvent A was aq. 0.1 % (v/v) trifluoroacetic acid and solvent B was acetonitrile containing 0.05 % (v/v) trifluoroacetic acid. The flow rate was 1.0 ml/min. The peptides were detected by UV at 230 nm. The molecular weight of each peptide was determined by an on-line mass spectrometry. The straight line represents the concentration of solvent B. All peptides which were eluted from the column were identified, and only the peptides with free Cys^{41}, disulfide bond between two Cys^{41}, and that between Cys^{41} and Cys^{149} are shown by arrows, which are accompanied by "41", "41-41", and "41-149", respectively.

Stability in the Presence of Reducing Reagent — To examine whether the cleavage of the disulfide bond formed between Cys^{41} and Cys^{149} influences the protein stability, the thermal denaturation curves for the wild-type protein, $A^{13}A^{63}$-TRNH[Δ150-161], and $A^{13}A^{41}A^{63}A^{149}$-TRNH[Δ150-161] were measured in the presence of 20 mM 2-Me. The addition of 2-Me decreased the stabilities of the wild-type protein and $A^{13}A^{63}$-TRNH[Δ150-161] by 6.3 and 6.9 °C in T_m (2.8 and 3.0 kcal/mol in ΔG_m), respectively (Table 1-2), but did not seriously affect the stability of $A^{13}A^{41}A^{63}A^{149}$-TRNH[Δ150-161]. These results suggest that the disulfide bond formed between Cys^{41} and Cys^{149} increases the protein stability by 6-7 °C in T_m and ~3 kcal/mol in ΔG_m.

Stabilities of the TRNH[Δ150-161] Variants at Cys^{149} — The mutation of Cys^{41} or Cys^{149} to Ala decreased the protein stability by ~9 °C in T_m and ~4 kcal/mol in ΔG_m, whereas the cleavage of the disulfide bond by the addition of 2-Me decreased it by only 6-7 °C in T_m and ~3 kcal/mol in ΔG_m. These results suggest that the thiol groups of these cysteine residues contribute to increase the protein stability by 2-3 °C in T_m and ~1 kcal/mol in ΔG_m. To clarify the mechanism, by which the thiol group increases the protein stability, mutant proteins of TRNH[Δ150-161], in which Cys^{149} was replaced by several other amino acid residues, were constructed and their thermal denaturations were analyzed. The results are summarized in Table 1-2. The decrease in the protein stability by the mutation of Cys^{149} to Val, Thr, or Ile (5-6 °C in T_m and 2.2-2.6 kcal/mol in ΔG_m) was comparable to that due to the cleavage of the disulfide bond, whereas the decrease in the protein stability by the mutation of Cys^{149} to Ser (7.8 °C in T_m and 3.4 kcal/mol in ΔG_m) was comparable to that due to the mutation of Cys^{149} to Ala. A characteristic common to the structures of Val, Thr, and Ile is that they have nonpolar methyl groups at the γ position. Therefore, these results suggest that the thiol group of Cys^{149} can be replaced by a methyl group without seriously affecting the protein stability. The thiol group of Cys^{149} may contribute to the protein stability by 2-3 °C in T_m and ~1 kcal/mol in ΔG_m by a hydrophobic effect. The enzymatic activities of these TRNH[Δ150-161]

derivatives ranged from 87 % to 168 % of that of TRNH[Δ150-161]. It remains to be determined why all of these mutant proteins, except for A^{149}-TRNH[150-161], are more active than TRNH[Δ150-161] .

1. 4 Discussion

Stabilization Mechanisms of T. thermophilus RNase HI — It has previously been shown that the sum of the local stabilizing forces or interactions, which are independent of one another, account for half of the difference in the in vitro stability between the *T. thermophilus* and *E. coli* RNases HI (9, 12). In this study, I showed that a disulfide bond formed between Cys^{41} and Cys^{149} account for 6-7 °C, which is roughly one-fifth of the difference in the in vitro stability between these proteins. Since the T_m value of *E. coli* RNase HI is 52.0 °C at pH 5.5 in the presence of 1 M GdnHCl (12), the difference in the in vitro stability between *T. thermophilus* and *E. coli* RNases HI is 31.7 °C in T_m under these conditions. Therefore, the difference in the in vivo stability between these proteins must be ~25 °C in T_m. This means that sum of the stabilizing factors identified thus far (16 °C in T_m) (12) already accounts for two-thirds of the difference in the in vivo stability between these proteins, if the difference in the T_m values is compared. Further mutagenesis studies may allow us to identify additional interactions that can account for the remaining difference in the in vivo stability between these proteins.

Stabilization by Disulfide Bond — The disulfide bond is one of the structural elements of proteins. It is usually involved in protein stabilization (43), predominantly by reducing the entropy of the unfolded state of proteins (chain entropy effect) (44-46). It has been reported that the conformational entropy of the unfolded protein is decreased in proportion to the increase in the natural logarithm of the number of the residues in the loop forming disulfide bond (47, 48). I showed that the formation of the disulfide bond between Cys^{41} and Cys^{149} increased the protein stability by 6-7 °C in T_m. This value is comparable to those reported for the mutant proteins of T4 lysozyme, in which a single artificial disulfide bond was introduced into various positions, so that the sizes of the loop formed by the cross-link ranged from 27 to 155 amino acid residues (48). The formation of the disulfide bond between Cys^{41} and Cys^{149} in *T. thermophilus*

RNase HI did not seriously affect the enzymatic activity, suggesting that the formation of this disulfide bond does not seriously affect either the substrate binding or the conformation of the active-site. In fact, a model for the three-dimensional structure of *E. coli* RNase HI complexed with the substrate indicates that Arg^{41}, which is corresponding to Cys^{41} in *T. thermophilus* RNase HI, is not involved in the substrate-binding site (49).

Identification of a Disulfide Bond in $A^{13}A^{63}$-TRNH[Δ150-161] — Peptide mapping analysis is often used to identify a disulfide bond in a protein molecule. However, it is not straightforward if the protein contains both reduced and oxidized cysteine residues, as *T. thermophilus* RNase HI does, because the cysteine residues involved in the disulfide bond are rapidly exchanged with the reduced cysteine residues upon proteolysis. In this case, the reduced cysteine residues should be chemically modified by a thiol-blocking reagent to prevent the sulfhydryl/disulfide exchange reaction. However, Cys^{13} of *T. thermophilus* RNase HI in the native state, which should be a reduced form, was not effectively modified, probably because this residue is relatively well buried inside the protein molecule (data not shown). Therefore, I constructed $A^{13}A^{63}$-TRNH[Δ150-161], which contains only two cysteine residues at position 41 and 149, to provide conclusive evidence that a disulfide bond is formed between these residues. Identification of both the reduced and oxidized form of $A^{13}A^{63}$-TRNH[Δ150-161] by peptide mapping analysis (Fig. 1-6b) suggests that the disulfide bond between Cys^{41} and Cys^{149} is not formed in vivo, but is spontaneously formed in vitro during the purification process in the absence of a reducing reagent. A similar phenomenon has been observed for elongation factor Ts from *T. thermophilus* (50,51). An intermolecular disulfide bond, which contributes to increasing the thermal stability of this protein without seriously affecting the enzymatic activity (50), is not formed in vivo but is formed in vitro in the absence of a reducing reagent (51).

Possible Involvement of cis-trans Isomerization of Pro^{148} in the Formation of a Non-Cross-Linked Protein — It has been reported that *T. thermophilus* RNase HI exists in a reduced form in the absence of a reducing reagent and urea, when it was purified in the presence of 8 M urea (1). As analyzed by CD, the secondary structure of this protein is not denatured in the presence of 8 M urea (1). However, because the backbone structure of the C-terminal region of this protein has not been defined by crystallographic analysis (28), this region may be locally unfolded in the presence of 8 M urea, and kept unfolded even when urea is removed. Since this region starts from Pro^{148}, Pro^{148} may assume a *cis* conformation, and *cis-trans* isomerization of this residue may create structural disorder in this region, thereby disturbing the formation of a disulfide bond between Cys^{41} and Cys^{149}. It has been reported that *cis-trans* isomerization of Pro often creates an additional, very slow phase in the kinetic processes of protein unfolding and refolding (52-54). Crystallographic studies of the wild-type protein in an oxidized form, with a single disulfide bond between Cys^{41} and Cys^{149}, will be necessary to prove this hypothesis.

The existence of two forms of *T. thermophilus* RNase HI evokes a question as to whether the thermal denaturation curve previously measured represents that of the protein in a reduced form or oxidized form. However, because the thermal denaturation curve of the protein in a reduced form was nearly identical to that of the protein in an oxidized form (data not shown), the thermal denaturation curve of the protein in a reduced form must reflect that of the protein in an oxidized form. The thermal denaturation curve was measured by monitoring the change in the CD values as the temperature was increased. Therefore, the formation of the disulfide bond between Cys^{41} and Cys^{149} may be accelerated at high temperatures and completed prior to the initiation of thermal denaturation, probably due to a dramatic increase in the rate of *cis-trans* isomerization of Pro^{148}. In fact, the peptide mapping analysis for A^{13}A^{63}-TRNH[Δ150-161] indicated that the disulfide bond was fully formed between Cys^{41} and Cys^{149}, when the protein was thermally denatured (Fig. 1-6c).

Tolerance to C-terminal Truncations — There are two conflicting reports on the tolerance of *E. coli* RNase HI to the C-terminal truncations. Haruki *et al.* (30) have shown that the truncated proteins of *E. coli* RNase HI with Asn^{143} at the C-terminus (143-RNase HI) is functional, but that with Met^{142} at the C-terminus (142-RNase HI) is non-functional in vivo. Analyses for the production levels and biochemical properties of a series of the mutant proteins with C-terminal truncations have suggested that 142-RNase HI is non-functional in vivo because of a dramatic decrease in the protein stability. In addition, the truncated proteins with Asn^{143}, Thr^{145}, and Leu^{146} at the C-termini could not be purified in an amount sufficient for biochemical characterizations, because their production levels in cells were quite poor. In contrast, Goedken *et al.* (55) have shown that the truncated protein of *E. coli* RNase HI with Lys^{122} at the C-terminus (RNHΔE) can be overproduced in *E. coli* and purified from cells, although it is recovered in an insoluble form. This truncated protein is less stable than the intact protein and lost Mg^{2+}-dependent activity. However, despite of the fact that it does not contain His^{124} and Asp^{134}, which have been shown to be catalytically important (Page 4 Fig. 3) (56, 57), it exhibited Mn^{2+}-dependent activity. Because *T. thermophilus* RNase HI is more stable than *E. coli* RNase HI, it is expected that *T. thermophilus* RNase HI is functionally more tolerant to C-terminal truncations than is *E. coli* RNase HI. In fact, cellular production level of the truncated protein of *T. thermophilus* RNase HI with Ser^{143} at the C-terminus (TRNH[Δ144-161]) was almost identical with that of the wild-type protein, although half of the protein was recovered in an insoluble form after sonication lysis (Fig. 1-2). The truncated protein TRNH[Δ144-161] retains 45 % of the enzymatic activity of the wild-type protein and is still more stable than *E. coli* RNase HI by ~17 °C in T_m. Therefore, it would be informative to analyze the effect of the C-terminal truncations beyond the residues 143-161 on the stability and activity of *T. thermophilus* RNase HI.

Enzymatic Activities of Cys Mutants — The mutation of Cys^{13} to Ala considerably decreased the enzymatic activity of *T. thermophilus* RNase HI. It has previously been shown that this mutation increased the K_m value of *E. coli* RNase HI by 13.5 fold, but did not seriously alter its k_{cat} value (49), suggesting that this mutation impairs the substrate binding of *E. coli* RNase HI without seriously affecting the hydrolysis rate. Therefore, it is unlikely that Cys^{13} is involved in the catalytic function of *T. thermophilus* RNase HI. Instead, as proposed for Cys^{13} of *E. coli* RNase HI (49), the main chain carbonyl oxygen of this residue may be engaged in the substrate binding through hydrogen bonding. The mutation of Cys^{13} to Ala may affect the substrate binding of *T. thermophilus* RNase HI more profoundly than that of *E. coli* RNase HI and thereby decrease its enzymatic activity. It is notable that $A^{13}A^{41}A^{63}A^{149}$-TRNH[Δ150-161] is more active than the reduced form of $A^{13}A^{63}$-TRNH[Δ150-161] by ~50 % (Table 1-2). This observation is surprising, because both of the single mutations of Cys^{41} to Ala and Cys^{149} to Ala slightly decrease the enzymatic activity of TRNH[Δ150-161]. Since Cys^{41} is located relatively close to Cys^{13}, the decrease in the enzymatic activity caused by the mutation of Cys^{13} to Ala may be compensated, to some extent, by the conformational change caused by the mutation of Cys^{41} to Ala.

1. 5 Conclusion

In this chapter, I showed that none of the proline residue clustered in the C-terminal region of *T. thermophilus* RNase HI contributed to the thermal stability of the protein. However, a disulfide bond formed between Cys^{41} and Cys^{149} accounted for 6-7 °C in T_m and ~3 kcal/mol in ΔG_m. This disulfide bond was not formed in vivo, but was spontaneously formed in vitro during the purification process in the absence of a reducing reagent. These results suggest that the difference in the in vivo stability between *T. thermophilus* and *E. coli* RNases HI must be ~25 °C in T_m.

Chapter 2. Enhancement of *T. thermophilus* RNase HI Activity

Enhancement of the Enzymatic Activity of Ribonuclease HI from *Thermus thermophilus* HB8 with a Suppressor Mutation Method

2. 1 Introduction

In chapter 1, I have identified and extracted one of the factors that are responsible for the difference in the in vitro stability between *T. thermophilus* and *E. coli* RNases HI. In this chapter, to understand the stability-activity relationship of *T. thermophilus* RNase HI in more detail, I attempted to evolve its mutant enzymes with enhanced activity by using an in vitro evolution method.

In vitro evolution (directed evolution) is an efficient technique to engineer protein variants with altered functions. This technique has also been used to probe the relationships between stability and activity of enzymes. By using this method, the stability of *Bacillus subtilis* esterase was increased by 14°C in T_m, without any reduction in enzymatic activity at moderate temperature (13). Likewise, the enzymatic activities of *B. subtilis* subtilisin E (14) and horse heart myoglobin (15) were increased by 256-fold in k_{cat}/K_m and 24.7-fold in k_1 (rate constant for H_2O_2 oxidation of metmyoglobin), respectively, without any reduction in protein stability. In addition, mutant enzymes of *B. subtilis* subtilisin E (16) and *B. stearothermophilus* catalase I (17), in which both the activities and stabilities were increased, have been isolated. These results suggest that enzymes from mesophiles and moderate thermophiles are not optimized with respect to activity and stability. However, it remains to be determined whether this hypothesis is valid for the enzymes from hyperthermophiles. In fact, in vitro evolution of hyperthermostable indoleglyceryl phosphate synthase from an extreme thermophile *Sulfolobus solfataricus* generated mutant enzymes, which are more active at low temperatures but less stable than the wild-type enzyme (58). In order to get more information on the activity-stability relationships of hyperthermostable enzymes, I used a similar technique to isolate mutant

enzymes of *T. thermophilus* RNase HI with enhanced activity at moderate temperatures.

To isolate mutant enzymes of *T. thermophilus* RNase HI with enhanced activity generated by random mutagenesis, an appropriate selection system is required. Because a system to determine the RNase H activity by an in situ assay is not available, I decided to develop a genetic system. *E. coli* strain MIC3001 with the *rnhA*-339::cat and *rec*B270(Ts) mutations, which shows an RNase H-dependent temperature-sensitive (ts) growth phenotype (59), was used for this purpose. This strain would be effective to screen for functional RNase HI mutants in vivo, because the structural genes of Type 1 RNases H from *T. thermophilus* HB8 (3), *Saccharomyces cerevisiae* (60), *Crithidia fasciculata* (61), and *Trypanosoma brucei* (62), and Type 2 RNases H from *E. coli* (63), *Streptococcus pneumoniae* (64), and *Pyrococcus kodakaraensis* KOD1 (65) were successfully cloned by their ability to complement the ts phenotype of this strain. Because *T. thermophilus* RNase HI efficiently complements the ts phenotype of *E. coli* MIC3001, I need to construct a mutant enzyme first, which cannot or can only poorly complement the ts phenotype of *E. coli* MIC3001 due to a reduction in the enzymatic activity. Screening for second-site revertants would allow me to identify the amino acid substitutions that make this mutant enzyme functional in vivo. These amino acid substitutions are expected to increase the activity of the wild-type enzyme. By using a similar genetic method, It has previously been succeeded in identifying a number of mutations that increase the thermal stability of *E. coli* RNase HI (30). *E. coli* RNase HI complements the ts phenotype of *E. coli* MIC3001, whereas the truncated protein 142-RNase HI, which lacks the C-terminal 13 residues, cannot complement it due to a great reduction in the stability. Eight of eleven single amino acid substitutions that make 142-RNase HI functional in vivo enhanced the thermal stability of the wild-type enzyme.

2. 2 Experimental Procedures

Materials — [γ-^{32}P]ATP (>5000Ci/mmol) was obtained from Amersham.

Cells and Plasmids — *E. coli* MIC3001 (*F*, *sup*E44, *sup*F58, *lac*Y1 or Δ(*lac*IZY)6, *trp*R55, *gal*K2, *gal*T22, *met*B1, *hsd*R14(r_K^-, m_K^+), *rnh*-339::cat, *rec*B270) was previously constructed (59). Plasmid pBR322 were from Takara Shuzo Co., Ltd.

Plasmid Construction — Plasmid pBR600, which was used for the complementation assay, was constructed by the following procedures. The *rnhA* gene in plasmid pJAL700T was amplified by PCR using primers 1 and 4 as 5'- and 3'-primers, respectively, and primers 2 and 3 as 3'- and 5'-mutagenic primers, respectively, as described in Chapter 1 for the construction of the mutant *T. thermophilus* RNase HI proteins. The sequences of these primers are shown in Fig. 2-1. The sequence complementary to the 134th codon, which is represented by NNN in the sequence of primer 2, is CTG for Asp in this case. These sequences were designed to silently eliminate the *Mlu*I site encompassing the sequences coding for Lys^3-Val^5 and silently introduce the unique *Sst*II and *Mlu*I sites encompassing the sequences coding for Pro^1-Arg^2 and Glu^{131}-Val^{133}, respectively. After digestion by the *Eco*RI and *Hin*dIII, the PCR fragment was ligated into the *Eco*RI-*Hin*dIII sites of plasmid pBR322 to generate plasmid pBR600. The promoter for the *rnhA* gene in this plasmid remains to be determined. The plasmid pBR600 derivatives, which contain the mutant *rnhA* genes with a series of substitutions at codon 134, were constructed by the same procedures, except that primer 2 with a different sequence was used. The sequence of primer 2 was designed so that the GAC codon for Asp^{134} was changed to CAT for His, GAA for Glu, CAA for Gln, TCC for Ser, ACC for Thr, GTC for Val, ATC for Ile and CTC for Leu. The mutant enzymes of *T. thermophilus* RNase HI at Asp^{134} are designated as X^{134}-TRNH, and the mutant *rnhA* genes encoding these mutant enzymes are designated as *rnhA134X*, where X represents the amino acid residue substituted for Asp^{134}. Plasmid pJAL700TM and its derivatives for the overproduction of *T. thermophilus* RNase

HI and its mutants were constructed by replacing the small *Nde*I-*Sal*I fragment of pJAL700T with those of pBR600 (Fig. 2-1).

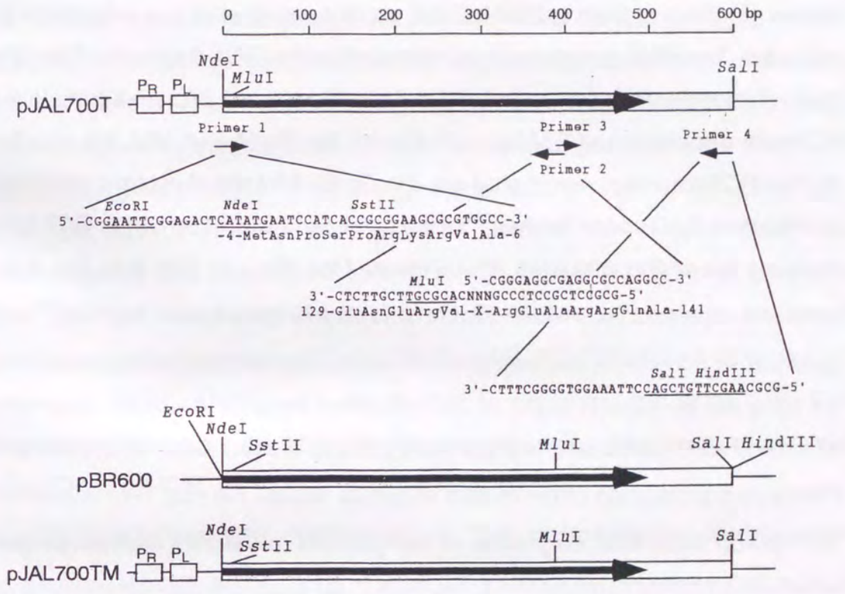

Fig. 2-1. Construction of plasmids pBR600 and pJAL700TM.
In plasmid pJAL700T, which was used as a template for PCR, the structural gene of *T. thermophilus* RNase HI (large arrow) is under the control of the bacteriophage λ promoters P_R and P_L. Nucleotide sequences together with amino acid sequences of the primers 1-4 (small arrows), which were used as 5'-, 3'-mutagenic, 5'-mutagenic, and 3'-primers for PCR, are indicated. *Numbers* in the amino acid sequences represent the positions of amino acids in the primary structure of *T. thermophilus* RNase HI.

Random Mutagenesis — Random point mutations were introduced into the 5'-terminal 400-bp DNA fragment of the *rnhA* gene by DNA shuffling method (66). This DNA fragment was first amplified from plasmid pBR600 by PCR using primers 1 and 2 (primer 2 with the GAC codon for the 134th residue) (Fig. 2-1). Taq DNA polymerase (Takara Shuzo Co., Ltd.), instead of Vent DNA polymerase, was used for it, because the fidelity of the former is lower than that of the latter. This DNA fragment was digested into the 50~100-bp fragments by DNase I in the presence of the Mg^{2+} ion, and then subjected to a primerless PCR using the Taq DNA polymerase to reassemble the DNA fragment. This DNA pool, obtained by the first round of DNA shuffling, was used as a template in PCR with primers 1 and 2. After digestion by the *Eco*RI and *Mlu*I, the resultant 400-bp PCR fragment was ligated into the *Eco*RI-*Mlu*I site of plasmid pBR600H, in which the GAC codon for Asp^{134} of the *rnhA* gene was changed to CAT for His. Because this codon is located downstream of the *Mlu*I site (Fig. 2-1), the mutant enzymes screened for second-site revertants always contain the Asp^{134}→His mutation, in addition to the mutations introduced by random mutagenesis. I did not carry out the second round of DNA shuffling, because desirable suppressor mutations were introduced into the *rnhA* gene by the first round of DNA shuffling. For the overproduction of the mutant enzymes without the Asp^{134}→His mutation, the 400-bp *Nde*I-*Mlu*I fragments of the plasmid pBR600H derivatives were substituted for the corresponding fragment in pJAL700TM. The plasmids for the overproduction of the single mutant enzymes A12S, K75M, and A77P, in which Ala^{12}, Lys^{75}, and Ala^{77} were replaced by Ser, Met, and Pro, respectively, were designated as pJAL12S, pJAL75M, and pJAL77P, respectively.

Screening for the mutant *rnhA* genes that complemented the ts phenotype of *E. coli* MIC3001 was carried out as described previously (57). *E. coli* MIC3001 cells were transformed with the plasmid pBR600H derivatives by electroporation using a Bio-Rad Gene Pulser, as described previously (67). The transformants were spread on two Luria-Bertani medium-agar plates with 5 g/liter NaCl and 50 mg/liter ampicillin, because the ts phenotype of MIC3001 is less pronounced at higher NaCl concentrations (59). One was incubated at

42 °C and the other was incubated at 30 °C. The colonies grown at 42 °C were selected and the plasmid pBR600H derivatives were isolated from each clone. After confirming that each plasmid suppressed the ts phenotype of *E. coli* MIC3001, the nucleotide sequences of the mutant *rnhA* genes were determined.

Combinations of Activating Mutations — Plasmid pJAL75M/77P for the overproduction of the double mutant enzyme $M^{75}P^{77}$-TRNH was constructed by site-directed mutagenesis using PCR. Primers 1 and 4 shown in Fig. 2-1 were used as 5'- and 3'-primers, respectively, and appropriate primers, instead of primers 2 and 3, were used as mutagenic primers. These mutagenic primers were designed so that the codon for Lys^{75} was changed from AAG to ATG for Met and the codon for Ala^{77} was changed from GCC to CCC for Pro. pJAL12S, pJAL75M, pJAL77P, and pJAL75M/77P contain the unique *Sac*I site encompassing the sequences coding for Glu^{48}-Leu^{49}. Therefore, plasmids pJAL12S/75M, pJAL12S/77P and pJAL12S/75M/77P for the overproduction of the double mutant enzymes $S^{12}M^{75}$-TRNH and $S^{12}P^{77}$-TRNH, and triple mutant enzyme $S^{12}M^{75}P^{77}$-TRNH were constructed by replacing the small *Sac*I-*Sal*I fragment of plasmid pJAL12S with the corresponding fragments of plasmid pJAL75M, pJAL77P, and pJAL75M/77P, respectively.

Overproduction and Purification — The overproducing strains were constructed by transforming *E. coli* HB101 with the plasmid pJAL700TM derivatives. Cultivation of these strains, and overproduction and purification of the mutant enzymes were carried out as described in Chapter 1 (68), except that all the purification procedures were carried out in the presence of 1 mM DTT.

RNase H Assay — The enzymatic activity was determined in 10 mM Tris-HCl (pH 8.0) containing 10 mM $MgCl_2$, 50 mM NaCl, 1 mM DTT, and 50 μg/ml bovine serum albumin at 30 or 60 °C by using a ^{32}P-labeled 29-bp DNA-RNA-DNA/DNA as a substrate. The 29-base DNA-RNA-DNA (5'-AATAGAGAAAAAGaaaaAAGATGGCAAAG-3'), in which DNA and RNA are

represented by uppercase and lowercase letters, respectively, and the 29-base DNA, which is complementary to this 29-base DNA-RNA-DNA, were kindly donated by ID Biomedical Corp. The preparation of the ^{32}P-labeled 29-bp DNA-RNA-DNA/DNA substrate and the quantitative analyses of the products separated with a 20 % polyacrylamide gel containing 7 M urea using a Instant Imager from Packard were carried out as described previously (65). One unit was defined as the amount of the enzyme producing 1 μmol of products per min. The specific activity was defined as the enzymatic activity/mg of protein. For the determination of the kinetic parameters, the concentration of the ^{32}P-labeled 29-bp DNA-RNA-DNA/DNA substrate was varied from 0.2 to 10 μM such that it spanned the K_m value. The amount of the enzyme was controlled carefully such that the fraction of the substrate hydrolyzed did not exceed 30 % of the total. In this condition, the amount of the product increased in proportion to the increase in the amount of the enzyme or the reaction time

Circular Dichroism Spectra — The measurements of CD spectra were carried out as described in Chapter 1, except that all of the CD spectra were measured at 30°C in 10 mM sodium acetate (pH 5.5) containing 0.1 M NaCl and 1 mM DTT.

Thermal Denaturation — The thermal denaturation curves and the temperature of the midpoint of the transition, T_m, were determined as described in Chapter 1, by monitoring the change in the CD value at 220 nm. The proteins were dissolved in 20 mM sodium acetate (pH 5.5) containing 1 M guanidine hydrochloride (GdnHCl) and 1 mM DTT. The protein concentration was approximately 0.13 mg/ml and a cell with an optical path length of 2 mm was used. The enthalpy change of unfolding at the T_m (ΔH_m) and the entropy change of unfolding at the T_m (ΔS_m) were calculated by van't Hoff analysis. The difference in the free energy change of unfolding between the mutant and wild-type proteins, at the T_m of the wild-type protein ($\Delta\Delta G_m$), was estimated by the relationship given by Becktel and Schellman (41), $\Delta\Delta G_m = \Delta T_m \cdot \Delta S_m$ (wild-type protein). The ΔS_m value of the wild-type protein was determined to be

0.269 kcal/(mol·K) from four independent experiments with errors of ±0.04 kcal/(mol·K). This value was used for the calculation of the $\Delta\Delta G_m$ values.

2. 3 Results

Mutations at Asp[134] — It has previously been shown that Asp[134] of *E. coli* RNase HI is involved in a catalytic function, but nine amino acid residues (Asn, His, Glu, Gln, Ser, Thr, Val, Ile, and Leu) are permissive at this position (57). All the resultant mutant enzymes retained the ability to complement the ts phenotype of *E. coli* MIC3001. However, the complementation abilities of these mutant enzymes, which were estimated from the sizes of the colonies of *E. coli* MIC3001 transformants grown at 42 °C, were correlated with the levels of their enzymatic activities. These results prompted me to examine whether the mutations at Asp[134] of *T. thermophilus* RNase HI equally reduce the catalytic activity of the enzyme and thereby reduce its complementation ability. All the amino acid residues that have been shown to be permissive at position 134 of *E. coli* RNase HI, except for Asn, were substituted for Asp[134] of *T. thermophilus* RNase HI, and the effects of these mutations on the complementation ability of the enzyme were analyzed. The effect of the Asp[134]→Asn mutation was not analyzed, because the N[134]-TRNH enzyme, in which Asp[134] is replaced by Asn, is expected to retain almost full activity, as did the *E. coli* RNase HI variant with this mutation (69). Interestingly, all the mutant enzymes, except for the H[134]-TRNH enzyme, in which Asp[134] was replaced by His, lost the complementation ability, suggesting that these mutant enzymes are not functional in vivo. The H[134]-TRNH enzyme retained low complementation ability, as compared to that of the wild-type enzyme. When *E. coli* MIC3001 transformants with pBR600 and pBR600H, in which the wild-type and H[134]-TRNH enzymes are produced, were grown on the plates at 42 °C for 18 h, the former formed colonies, whereas the latter did not. *E. coli* MIC3001 transformants with pBR600H formed colonies, only when they were grown at 42 °C for more than 24 h. I used the H[134]-TRNH enzyme for screening of second-site revertants.

Enzymatic Activity and Thermal Stability of H[134]-TRNH enzyme — To confirm that the reduction in the complementation ability of the H[134]-TRNH enzyme is due to the reduction in its catalytic activity, the enzymatic activity and thermal stability of the purified H[134]-TRNH enzyme were determined and compared with those of the wild-type enzyme. The kinetic parameters of the wild-type and H[134]-TRNH enzymes were determined at 30 °C using the 29-bp DNA-RNA-DNA/DNA substrate. This substrate is suitable to determine the kinetic parameters of the RNase HI enzymes, because it is cleaved by *E. coli* RNase HI at a unique position in the middle of the tetra-adenosines (65). *T. thermophilus* RNase HI and its variants constructed in this experiment also cleaved it at this position (data not shown). The results are summarized in Table 2-1. The Asp[134]→His mutation resulted in a large reduction in the k_{cat} value, along with a slight reduction in the K_m value. As the result, the catalytic efficiency (k_{cat}/K_m) of the H[134]-TRNH enzyme, which was only ~9 % of that of the wild-type enzyme, was decreased due to the reduction in the hydrolysis rate (k_{cat}).

Table 2-1
Kinetic Parameters of the Wild-type and H[134]-TRNH Enzymes

Enzyme	K_m (μM)	k_{cat} (min^{-1})	k_{cat}/K_m ($\mu M^{-1} \cdot min^{-1}$)	Relative k_{cat}/K_m
WT-TRNH	7.8	4.9	0.63	1.0
H[134]-TRNH	3.3	0.18	0.055	0.087

The enzymatic activity was determined at 30°C for 15 min in 10 mM Tris-HCl (pH 8.0) containing 10 mM $MgCl_2$, 50 mM NaCl, 50 μg/ml bovine serum albumin, and 1 mM DTT, by using ^{32}P-labeled 29-bp DNA-RNA-DNA/DNA as a substrate. The kinetic parameters were determined by a least-squares fit of the data obtained from the Lineweaver-Burk plots. The relative k_{cat}/K_m was calculated by dividing the k_{cat}/K_m value of the mutant enzyme by that of the wild-type enzyme. Errors are within 30 % for the K_m and k_{cat} values reported, which are the averages of two independent experiments.

The thermal denaturation curves of the wild-type and H^{134}-TRNH enzymes were measured by monitoring the change in the CD values at 220 nm at pH 5.5 in the presence of 1 M GdnHCl and 1 mM DTT. Both enzymes were shown to unfold reversibly in a single cooperative fashion under this condition (data not shown). The thermodynamic parameters of these enzymes are summarized in Table 2-2. The T_m value of the wild-type enzyme (77.4°C) was identical with that determined in Chapter 1 at pH 5.5 in the presence of 1 M GdnHCl and 20 mM 2-mercaptoehtanol, suggesting that the thermal denaturation curve of the wild-type enzyme obtained in this experiment represents that of the enzyme in a reduced form. The H^{134}-TRNH enzyme was more stable than the wild-type enzyme by 2.0 °C in T_m and 0.5 kcal/mol in ΔG_m, suggesting that the $Asp^{134}\rightarrow$His mutation is not unfavorable for the conformational stability. The far-UV CD spectrum of the D134H enzyme was basically identical with that of the wild-type enzyme, suggesting that the protein conformation is not markedly changed by the mutation.

Table 2-2
Thermodynamic Parameters of the Wild-type and H^{134}-TRNH Enzymes

Enzyme	T_m (°C)	ΔT_m (°C)	ΔH_m (kcal/mol)	$\Delta\Delta G_m$ (kcal/mol)
WT-TRNH	77.4		94	
H^{134}-TRNH	79.4	2.0	101	0.5

The ΔS_m value of the wild-type protein was determined to be 0.269 kcal/(mol·K) from four independent experiments with errors of ±0.04 kcal/(mol·K). Errors are the same as those described in the legend for Table 1-1.

Screening for Suppressor Mutations — The screening for second-site revertants of a mutant protein often results in the reversion of the original point mutation, rather than yielding true second-site reversions. Therefore, random mutagenesis was introduced into the upstream region of the codon 134 in the *rnhA134H* gene, to avoid the reversion of the original point mutation at the codon 134. This region encompasses the sequences encoding amino acid residues at positions 7-128 (Fig. 2-1). When *E. coli* MIC3001 transformants were examined for their growth at 42 °C, the transformants which form colonies in 18 h, were obtained with a frequency of $1/10^4$. Plasmid DNAs were isolated from 10 colonies grown at 42 °C (strains 1-10) and the DNA sequences of the mutant *rnhA134H* genes were determined. The results are summarized in Table 2-3. Strains 2 and 10 produced the same variant of the H^{134}-TRNH enzyme with single $Ala^{77}\rightarrow$Pro mutation. Likewise, strains 5 and 8 produced the H^{134}-TRNH enzyme variants with single $Lys^{75}\rightarrow$Met and $Ala^{12}\rightarrow$Ser mutations, respectively. Other strains produced the H^{134}-TRNH enzyme variants with double and quadruple mutations, in which either the $Ala^{12}\rightarrow$Ser, $Lys^{75}\rightarrow$Met, or $Ala^{77}\rightarrow$Pro mutation is always included. The complementation levels of the enzyme variants with double or quadruple mutations were similar to or below those of the enzyme variants with single mutations. These results strongly suggest that, of the eleven mutations isolated in this experiment, only the $Ala^{12}\rightarrow$Ser, $Lys^{75}\rightarrow$Met, or $Ala^{77}\rightarrow$Pro mutation can suppress the effect of the $Asp^{134}\rightarrow$His mutation on the complementation ability of the enzyme. To analyze the effects of these mutations on the activity and stability of the wild-type enzyme, the mutant enzymes with these suppressor mutations alone were constructed, purified to give a single band on SDS-PAGE, and characterized for activities and stabilities. I have not purified and biochemically characterized the mutant enzymes with both suppressor and $Asp^{134}\rightarrow$His mutations.

Table 2-3

Complementation Levels of the Revertants of the H^{134}-TRNH Enzyme and Mutations Contained in these Revertants

Strain number	Complementation level	Mutations with amino acid substitutions	Mutations without amino acid substitutions
#1	+ +	$Ala^{12} \rightarrow Ser(\underline{G}CC \rightarrow \underline{T}CC)$	$Ala^{52}(GC\underline{C} \rightarrow GC\underline{T})$
		$Lys^{122} \rightarrow Arg(A\underline{A}G \rightarrow A\underline{G}G)$	$Val^{116}(GT\underline{G} \rightarrow GT\underline{A})$
#2	+ +	$Ala^{77} \rightarrow Pro(\underline{G}CC \rightarrow \underline{C}CC)$	$Cys^{13}(TG\underline{C} \rightarrow TG\underline{T})$
#3	+	$Ala^{12} \rightarrow Ser(\underline{G}CC \rightarrow \underline{T}CC)$	$Glu^{48}(GA\underline{G} \rightarrow GA\underline{A})$
		$Leu^{35} \rightarrow Pro(C\underline{T}C \rightarrow C\underline{C}C)$	
		$Ala^{93} \rightarrow Val(G\underline{C}G \rightarrow G\underline{T}G)$	
		$Arg^{117} \rightarrow Cys(\underline{C}GC \rightarrow \underline{T}GC)$	
#4	+	$Lys^{75} \rightarrow Met(A\underline{A}G \rightarrow A\underline{T}G)$	
		$His^{119} \rightarrow Tyr(\underline{C}AC \rightarrow \underline{T}AC)$	
#5	+ +	$Lys^{75} \rightarrow Met(A\underline{A}G \rightarrow A\underline{T}G)$	$Leu^{25}(CT\underline{C} \rightarrow CT\underline{T})$
#6	+ +	*$Ala^{40} \rightarrow Pro(\underline{G}CC \rightarrow \underline{C}CC)$*	$Leu^{25}(CT\underline{C} \rightarrow CT\underline{T})$
		$Lys^{75} \rightarrow Met(A\underline{A}G \rightarrow A\underline{T}G)$	$Ala^{93}(GC\underline{G} \rightarrow GC\underline{A})$
#7	+	*$Glu^{64} \rightarrow Gly(G\underline{A}G \rightarrow G\underline{G}G)$*	$Leu^{25}(CT\underline{C} \rightarrow CT\underline{T})$
		$Ala^{77} \rightarrow Pro(\underline{G}CC \rightarrow \underline{C}CC)$	
#8	+ +	$Ala^{12} \rightarrow Ser(\underline{G}CC \rightarrow \underline{T}CC)$	
#9	+	$Lys^{75} \rightarrow Met(A\underline{A}G \rightarrow A\underline{T}G)$	
		$Glu^{105} \rightarrow Gly(G\underline{A}G \rightarrow G\underline{G}G)$	
#10	+ +	$Ala^{77} \rightarrow Pro(\underline{G}CC \rightarrow \underline{C}CC)$	$Phe^{28}(TT\underline{C} \rightarrow TT\underline{T})$

Complementation level was estimated from the size of the colonies of *E. coli* MIC3001 transformants at 42 °C ("++" for large and "+" for medium sizes). *E. coli* MIC3001 transformants with plasmid pBR600 gave large colonies, whereas those with plasmid pBR600H gave small colonies. The codons with mutations are shown in parentheses, in which underlines represent the substituted nucleotides. The mutations, which alone may not be able to improve the complementation ability of the H^{134}-TRNH enzyme, are shown in *italics*.

Enzymatic activities of Mutant Enzymes — The kinetic parameters of the mutant enzymes, in which suppressor mutations were individually introduced or combined, were determined at 30 °C using the 29-bp DNA-RNA-DNA/DNA substrate and compared with those of the wild-type enzyme. The results are summarized in Table 2-4. The $Ala^{12} \rightarrow Ser$ mutation decreased the K_m value by 5.2 fold without seriously affecting the k_{cat} value. The $Lys^{75} \rightarrow Met$ mutation increased the k_{cat} value by 1.6 fold without seriously affecting the K_m value. The $Ala^{77} \rightarrow Pro$ mutation decreased the K_m value by 2.4 fold and increased the k_{cat} value by 1.5 fold. Accordingly, all of these mutations increased the k_{cat}/K_m value of the wild-type enzyme by 2.1-4.8 fold. These results indicate that all the suppressor mutations, which restored normal complementation ability to the H^{134}-TRNH enzyme, enhanced the catalytic efficiency of the wild-type enzyme at moderate temperatures. Combination of these suppressor mutations generated more active mutant enzymes with the k_{cat}/K_m values that were higher than that of the wild-type enzyme by 16-40 fold (Table 2-4). Of them, the $S^{12}M^{75}P^{77}$-TRNH enzyme, which contain all three suppressor mutations, exhibited the highest catalytic efficiency. For the multiple mutant enzymes, hypothetical relative k_{cat}/K_m values were obtained by assuming that each effect of suppressor mutation on the enzymatic activity was independent and cumulative. The results indicated that the k_{cat}/K_m values of all the multiple mutant enzymes were higher than their hypothetical values, but only by at most 2 fold, mainly due to the cooperative increases in their k_{cat} values. Thus, the each effect of suppressor mutation on the enzymatic activity was roughly cumulative, while all the combinations created cooperative effect on the hydrolysis rate.

To examine whether the mutant enzymes with suppressor mutations are more active than the wild-type enzyme at elevated temperatures as well, the specific activities of the wild-type and $S^{12}M^{75}P^{77}$-TRNH enzymes were determined at 30 and 60 °C using the 29-bp DNA-RNA-DNA/DNA substrate (Table 2-5). This triple mutant enzyme was chosen as a representative of the mutant enzymes, because it showed the highest activity. The specific activity of

this mutant enzyme was higher than that of the wild-type enzyme by ~20 fold both at 30 and 60 °C, suggesting that combination of three suppressor mutations enhanced the enzymatic activity of *T. thermophilus* RNase HI at its optimum temperature. The optimum temperature of *T. thermophilus* RNase HI has not been determined, because the duplex form of the substrate is denatured at the temperatures higher than 70 °C.

Table 2-4
Kinetic Parameters of the Wild-type and Mutant Enzymes

Enzyme	K_m (μM)	k_{cat} (min^{-1})	k_{cat}/K_m ($\mu M^{-1} \cdot min^{-1}$)	Relative k_{cat}/K_m	Hypothetical relative k_{cat}/K_m
WT-TRNH	7.8	4.9	0.63	1.0	1.0
S^{12}-TRNH	1.5	4.5	3.0	4.8	
M^{75}-TRNH	6.1	8.0	1.3	2.1	
P^{77}-TRNH	3.3	7.3	2.2	3.5	
$S^{12}M^{75}$-TRNH	1.1	12	11	17	10
$S^{12}P^{77}$-TRNH	1.3	15	12	19	17
$M^{75}P^{77}$-TRNH	2.0	20	10	16	7.4
$S^{12}M^{75}P^{77}$-TRNH	1.1	27	25	40	35

The enzymatic activities and kinetic parameters of the wild-type and mutant enzymes were determined as described in the legend for Table 2-1. Hypothetical relative k_{cat}/K_m values were calculated by multiplying the relative k_{cat}/K_m values of the single mutant enzymes with constituent substitutions. Errors are the same as those described in the legend for Table 2-1.

Table 2-5
Comparison of Specific Activities of the Wild-type and $S^{12}M^{75}P^{77}$-TRNH Enzymes

Enzyme	Temperature (°C)	Specific activity (U/mg)	Relative activity
WT-TRNH	30	0.029	1.0
	60	0.78	27
$S^{12}M^{75}P^{77}$-TRNH	30	0.59	20
	60	15	517

Specific activities were determined at 30 and 60 °C for 15 min by using ^{32}P-labeled 29-bp DNA-RNA-DNA/DNA as a substrate under the conditions described under legend for Table 1. The enzymes and substrates were preincubated for 5 min at designated temperatures. One unit was defined as the amount of the enzyme producing 1 μmol of products. The concentration of substrate was 1 μM. Errors are the same as those described in the legend for Table 2-1.

Thermal stability — To analyze the effects of the suppressor mutations on the protein stability, the thermal denaturation curves were measured by monitoring the change in the CD values at 220 nm (Fig. 2-2). All mutant enzymes were shown to reversibly unfold in a single cooperative fashion. The thermodynamic parameters of these mutant enzymes, which were obtained by assuming that these enzymes unfold in a two state mechanism, are summarized in Table 2-6. Of the single mutant enzymes, only the P^{77}-TRNH enzyme was considerably less stable than the wild-type enzyme by 5.7°C in T_m and 1.5 kcal/mol in ΔG_m, indicating that the $Ala^{77} \rightarrow Pro$ mutation considerably decreased the protein stability, whereas other mutations did not seriously affect it. However, the $M^{75}P^{77}$-TRNH and $S^{12}M^{75}P^{77}$-TRNH enzymes, which contain both the $Lys^{75} \rightarrow Met$ and $Ala^{77} \rightarrow Pro$ mutations, were less stable than the wild-type enzyme only by 1.8 and 2.4°C in T_m and 0.5 and 0.7 kcal/mol in ΔG_m, respectively. These results suggest that the destabilization effect of the $Ala^{77} \rightarrow Pro$ mutation is compensated by the $Lys^{75} \rightarrow Met$ mutation, which does not seriously affect the protein stability by itself. The $Ala^{12} \rightarrow Ser$ mutation did not compensate this destabilization effect, because the $S^{12}P^{77}$-TRNH enzyme was less stable than the wild-type enzyme by 6.4°C in T_m and 1.7 kcal/mol in ΔG_m. To evaluate the cooperative effects of the $Lys^{75} \rightarrow Met$ and $Ala^{77} \rightarrow Pro$ mutations on the protein stability more quantitatively, the hypothetical $\Delta\Delta G_m$ values were calculated for the multiple mutant enzymes by simply adding the $\Delta\Delta G_m$ values of the single mutant enzymes with constituent substitutions (Table 2-6). The $\Delta\Delta G_m$ values of the $S^{12}M^{75}$-TRNH and $S^{12}P^{77}$-TRNH enzymes were almost identical with the hypothetical values. In contrast, The $\Delta\Delta G_m$ values of the $M^{75}P^{77}$-TRNH and $S^{12}M^{75}P^{77}$-TRNH enzymes were higher than the hypothetical values by ~1 kcal/mol in ΔG_m.

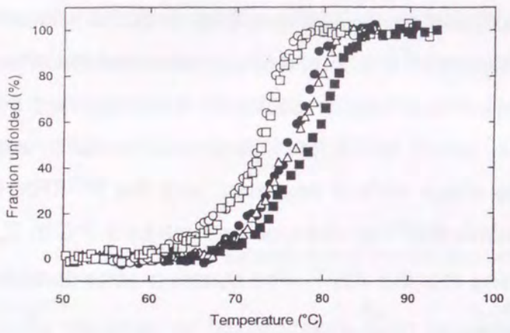

Fig. 2-2. Thermal denaturation curves of the wild-type and mutant enzymes.
The apparent fraction of unfolded protein is shown as a function of temperature. Thermal denaturation curves of the wild-type and all of the mutant enzymes were determined at pH 5.5 in the presence of 1 M GdnHCl and 1 mM DTT by monitoring the change in the CD value at 220 nm, as described under "Experimental Procedures". The curves of the wild-type (■), P^{77}-TRNH (□), $S^{12}P^{77}$-TRNH (○), $M^{75}P^{77}$-TRNH (△), and $S^{12}M^{75}P^{77}$-TRNH (●) enzymes are shown as representatives.

Table 2-6
Thermodynamic Parameters of the Wild-type and Mutant Enzymes

Enzyme	T_m (°C)	ΔT_m (°C)	ΔH_m (kcal/mol)	$\Delta\Delta G_m$ (kcal/mol)	Hypothetical $\Delta\Delta G_m$ (kcal/mol)[a]
WT-TRNH	77.4		94		
S^{12}-TRNH	76.0	-1.4	86	-0.4	
M^{75}-TRNH	78.2	0.8	93	0.2	
P^{77}-TRNH	71.7	-5.7	77	-1.5	
$S^{12}M^{75}$-TRNH	76.8	-0.6	103	-0.2	-0.2
$S^{12}P^{77}$-TRNH	71.0	-6.4	87	-1.7	-1.9
$M^{75}P^{77}$-TRNH	75.6	-1.8	90	-0.5	-1.3
$S^{12}M^{75}P^{77}$-TRNH	75.0	-2.4	100	-0.7	-1.7

Errors are the same as those described in the legend for Table 1-1.
[a]Hypothetical $\Delta\Delta G_m$ values represent the sum of the $\Delta\Delta G_m$ values of the single mutant enzymes with constituent substitutions.

CD spectra — The far-UV CD spectra of all mutant enzymes, except for those of the $M^{75}P^{77}$-TRNH and $S^{12}M^{75}P^{77}$-TRNH enzymes, were indistinguishable from that of the wild-type enzyme (data not shown). All spectra gave a broad trough with the minimum [θ] value of ~-12,500 around 210-215 nm. However, the spectra of the $M^{75}P^{77}$-TRNH and $S^{12}M^{75}P^{77}$-TRNH enzymes, which were similar with each other, were different from that of the wild-type enzyme in the 220-235 nm region (Fig. 2-3a). In this region, the former spectra were sharper than the latter spectrum. As a result, the former spectra gave another small minimum with the [θ] value of ~-2,500 at 235 nm, whereas the latter spectrum did not. This difference may be produced by conformational changes of the aromatic residues, because the spectrum of the $M^{75}P^{77}$-TRNH or $S^{12}M^{75}P^{77}$-TRNH enzyme in the 200-220 nm region, which reflects the content of the secondary structures of the protein, is similar to that of the wild-type enzyme, and because a positive contribution of the tryptophan residue to the CD spectrum at 228 nm has been reported (70). In fact, the near-UV CD spectra of the $M^{75}P^{77}$-TRNH and $S^{12}M^{75}P^{77}$-TRNH enzymes, which reveals the three-dimensional environments of the aromatic residues, were slightly different from that of the wild-type enzyme (Fig. 2-3b), whereas those of other mutant enzymes were basically the same as that of the wild-type enzyme (data not shown). These results suggest that the simultaneous introduction of the Lys^{75}→Met and Ala^{77}→Pro mutations causes a local conformational change, but only to a small extent. Thus, all of three suppressor mutations and their combinations did not seriously affect the overall structure of the enzyme.

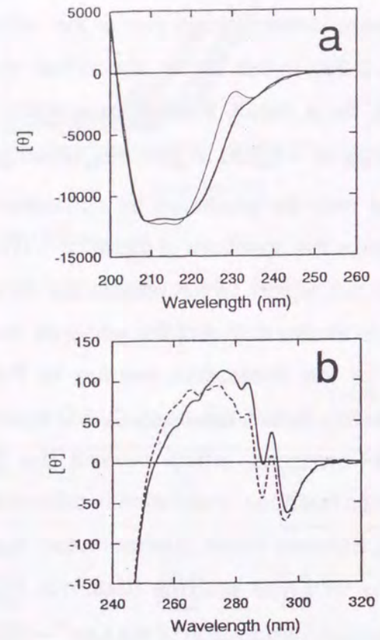

Fig. 2-3. CD spectra of the wild-type and mutant enzymes.
The CD spectra of the wild-type and all mutant enzymes were measured as described under "Experimental Procedures". (a) The far-UV CD spectrum of the $M^{75}P^{77}$-TRNH enzyme (thin line) is shown in comparison with that of the wild-type enzyme (thick line). The far-UV CD spectrum of the $S^{12}M^{75}P^{77}$-TRNH enzyme is basically the same as that of the $M^{75}P^{77}$-TRNH enzyme. The far-UV CD spectra of all other mutant enzymes are basically the same as that of the wild-type enzyme. (b) The near-UV CD spectrum of the $S^{12}M^{75}P^{77}$-TRNH enzyme (broken line) is shown in comparison with that of the wild-type enzyme (thick line). The near-UV CD spectrum of the $M^{75}P^{77}$-TRNH enzyme is similar to that of the $S^{12}M^{75}P^{77}$-TRNH enzyme, whereas those of other mutant enzymes are similar to that of the wild-type enzyme.

2. 4 Discussion

Strategy to Enhance Enzymatic Activity — In this study, I employed suppressor mutation methods to improve the enzymatic activity of *T. thermophilus* RNase HI. This method includes complementation of the RNase H-dependent ts phenotype of *E. coli* MIC3001. Of the eight mutant enzymes, in which Asp^{134} was replaced by various amino acid residues, only the H^{134}-TRNH enzyme complemented the ts phenotype of *E. coli* MIC3001, but with poor efficiency. Because the enzymatic activity of the H^{134}-TRNH enzyme must be close to the critical level of RNase H activity, which is required to complement the ts phenotype of *E. coli* MIC3001, a slight increase in the enzymatic activity would be sufficient to improve the complementation ability of this mutant enzyme. In fact, screening for the second-site revertants of the H^{134}-TRNH enzyme allowed me to isolate three suppressor mutations that improved the catalytic efficiency of the wild-type enzyme only by 2.1-4.8 fold. In contrast, attempts to isolate second-site revertants of other mutant enzymes, such as E^{134}-TRNH and Q^{134}-TRNH, have been so far unsuccessful (data not shown). In addition, none of the suppressor mutations of the H^{134}-TRNH enzyme were sufficient to make these mutant enzymes functional in vivo, even when all of them were combined (data not shown). Therefore, the enzymatic activities of other mutant enzymes must be lower than the critical level by more than 40 fold. These results are consistent with the previous ones that the Asp^{134}→His mutation reduced the enzymatic activity of *E. coli* RNase HI only by 40 %, whereas other mutations dramatically reduced it by more than 100 fold (57). The complementation abilities of the *T. thermophilus* RNase HI variants were always lower than those of the corresponding *E. coli* RNase HI variants, probably because the enzymatic activity of *T. thermophilus* RNase HI in the *E. coli* cells is much lower than that of *E. coli* RNase HI.

Ala[12]→Ser Mutation — The Ala[12]→Ser mutation improved the affinity of the enzyme for the substrate, without seriously affecting the hydrolysis rate and thermal stability of the enzyme. Ala[12] is located in the βA-strand and exposed to the solvent (Fig. 2-4a). This residue is replaced by Ser in *E. coli* RNase HI. Because other residues around this residue from Phe[8] to Gly[21] are fully conserved in *E. coli* RNase HI, the Ala[12]→Ser mutation makes the sequence of a peptide segment from Phe[8] to Gly[21] identical with that of *E. coli* RNase HI. Structural and mutational studies of *E. coli* RNase HI revealed that Asp[10], Glu[48], Asp[70], His[124], and Asp[134] form the active-site (24). According to the latest model for the catalytic mechanism of the enzyme (Page 4 Fig. 3) (71), His[124] accepts a proton from an attacking H_2O molecule that acts as a general base. Asp[134] hold this H_2O molecule. Glu[48] anchors the H_2O molecule that acts as a general acid. Asp[10], as well as the main chain carbonyl oxygen of Gly[11], provide coordinating groups for binding of the catalytically-essential Mg^{2+} ion. Asp[70] governs the conformation of Asp[10]. In addition, a large cleft-like depression, which extends from the negatively charged active-site to the positively charged αIII-helix and the following loop, has been proposed to form the substrate binding site (24). Cys[13], Asn[16], Thr[43], Asn[44], and Asn[45] located in this depression have been shown to be involved in substrate binding (49). All of these residues involved in the catalytic function and substrate binding are conserved in *T. thermophilus* RNase HI. Of them, Asp[10], Gly[11], Cys[13], and Asn[16] are located in a peptide segment from Phe[8] to Gly[21]. Therefore, it seems likely that the Ala[12]→Ser mutation causes a conformational change, which is favorable for the amino acid residues involved in the substrate binding. This conformational change must be subtle, because the far- and near-UV CD spectra of the S[12]-TRNH enzyme were almost identical with those of the wild-type enzyme. It is unlikely that Ser[12] of the S[12]-TRNH enzyme forms a hydrogen bond with the substrate and thereby improves the affinity of this mutant enzyme for the substrate, because the substrate titration experiment using NMR previously indicated that Ser[12] of *E. coli* RNase HI is not directly involved in the substrate binding (49).

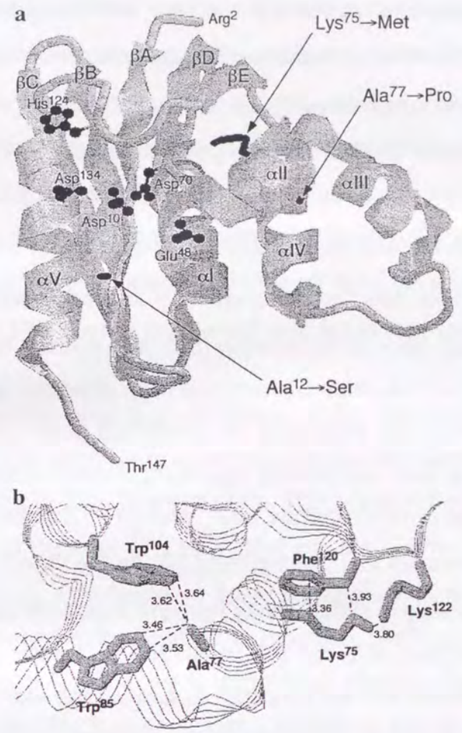

Fig. 2-4. Three-dimensional structure of *T. thermophilus* RNase HI.
(a) The backbone structure of *T. thermophilus* RNase HI, determined by Ishikawa *et al.* (28), was drawn with the program RasMol. Arg[2] and Thr[147] represent the N- and C-terminal residues in this crystal structure, because the N-terminal region from Met[-4] to Pro[1] and the C-terminal region from Pro[148] to Ala[161] have not been defined by crystallographic analyses, probably due to structural disorder. The side chains of Ala[12], Lys[75], and Ala[77], as well as the types of the amino acid substitutions that enhance the catalytic efficiency of the enzyme, are indicated. In addition, the side chains of the active-site residues (Asp[10], Glu[48], Asp[70], His[124], and Asp[134]) are shown. (b) The backbone structure around Lys[75] and Ala[77] is shown. The side chains of these residues, as well as those of Trp[85], Trp[104], Phe[120], and Lys[122] are shown. The *numbers* indicate atomic distance (Å). This crystal structure of *T. thermophilus* RNase HI has been deposited in the Brookhaven Protein Data Bank under accession number 1RIL.

Lys^{75}→Met and Ala^{77}→Pro Mutations — The Lys^{75}→Met mutation increased the hydrolysis rate of the enzyme, without seriously affecting the affinity for the substrate and stability of the enzyme. In contrast, the Ala^{77}→Pro mutation increased both the hydrolysis rate and affinity for the substrate of the enzyme, but at a cost of protein stability. Neither mutation seriously affected the protein structure. Lys^{75} and Ala^{77}, which correspond to Arg^{75} and Gly^{77} of *E. coli* RNase HI, respectively, are located in the αII-helix, which extends from Tyr^{73} to Glu^{80} (Fig. 2-4a). This helix, together with αI- and αIV-helices and βE-strand, form a hydrophobic core of the protein (28). In addition, this helix has been proposed to form the substrate-binding site (49), although none of the specific interactions between this helix and substrate has been identified. Thus, this helix is structurally and functionally important. Nevertheless, six of the eight residues in this helix, which include Leu^{74} and Phe^{78} that form the hydrophobic core, are not conserved in *E. coli* RNase HI. As the result, the αII-helix of *T. thermophilus* RNase HI is shifted away from the molecular center by more than 1 Å as compared to that of *E. coli* RNase HI (28). This shift has been suggested to be one of the factors that are responsible for the high stability and low activity of *T. thermophilus* RNase HI at moderate temperatures as compared to those of *E. coli* RNase HI (28).

Lys^{75} is exposed to the solvent, although the methylene groups in the side chain of this residue seem to make hydrophobic contacts with Phe^{120} (Fig. 2-4b). In addition, this amino group probably makes an electrostatic interaction with that of Lys^{122} (Fig. 2-4b). Phe^{120} and Lys^{122} are located in the βE-strand (Fig. 2-4a). The loop following this β-strand contains His^{124}. Because it has been suggested that the flexibility of this loop is important to position His^{124} to catalyze the hydrolytic reaction (28), the Lys^{75}→Met mutation may alter the interaction between the βE-strand and αII-helix and thereby induces a favorable conformational change of His^{124}. The Lys^{75}→Met mutation did not seriously affect the protein stability, probably because the positive-charge repulsion

between Lys^{75} and Lys^{122} does not contribute the protein stability.

Ala^{77} is almost fully buried inside the protein molecule. The Ala^{77}→Pro mutation destabilized the protein, probably due to the intrinsic destabilization of the αII-helix by the introduction of the proline residue. Because this helix is involved in a putative substrate-binding site and located close to the active-site, slight conformational change of this helix may induce favorable conformational changes of both active-site and substrate binding site. It has previously been reported that conformational difference in the αII-helix between *T. thermophilus* and *E. coli* RNases HI accounts for a small shift of the side-chain of Asp^{70} (28).

Cooperativity in the Effects of Mutations — The effect of each mutation on enzymatic activity are roughly cumulative, but all the combinations show a cooperative increase in the hydrolysis rate. This cooperative increase may be caused by the introduction of Lys^{75}→Met or Ala^{77}→Pro mutations, which increase the hydrolysis rate, because these mutations may induce the favorable conformational changes of the active-site residues, His^{124} or Asp^{70}. In addition, since the backbone of Ala^{12} connects with that of catalytic residue, Asp^{10}, there is a possibility that the Ala^{12}→Ser mutation combined with other mutations may also induce a favorable conformational change of the active-site, despite the fact that this mutation alone does not seriously affect the hydrolysis rate. Therefore, persisting conformational changes of active-site may account for the cooperative increase in the hydrolysis rate, when each suppressor mutation is combined with each other.

The effects of the Lys^{75}→Met and Ala^{77}→Pro mutations on protein stability, as well as those on protein conformation, are cooperative and not simply independent. These cooperative effects of the mutations are not surprising, because Lys^{75} and Ala^{77} are located close to each other. The CD spectra shown in Fig. 2-3 suggest that the conformations of the aromatic residues are altered, only when these mutations are simultaneously introduced. In the vicinity of Ala^{77}, two tryptophan residues (Trp^{85} and Trp^{104}) are located (Fig. 2-4b). In addition,

Tyr[73], Trp[81], and Trp[90] are located around this region. Therefore, it seems likely that the conformation of the αII-helix was significantly changed when the Lys[75]→Met and Ala[77]→Pro mutations were simultaneously introduced and this change forced these aromatic residues to change their configurations. The elimination or introduction of the interactions that specified this conformational change remained to be determined. However, this conformational change is favorable for protein stability, because the M[75]P[77]-TRNH enzyme was more stable than the P[77]-TRNH enzyme by 3.9 °C in T_m and 1.0 kcal/mol in ΔG_m.

Stability – Activity Relationships — In this study, I showed that the enzymatic activities of *T. thermophilus* RNase HI at both low and high temperatures were improved without a cost of protein stability. This result suggests that hyperthermophilic enzymes are not optimized in their activities even at their physiological conditions. Then the question arises whether an increase in the enzymatic activity of *T. thermophilus* RNase HI is accompanied by an increase in the conformational flexibility. It has previously been shown that the thermal stability of *E. coli* RNase HI could be improved without serious loss of enzymatic activity (12). Hydrogen-deuterium exchange analyses of the *E. coli* RNase HI variant, which is more stable than the wild-type protein by 20.2°C in T_m, have shown that an increase in stability does not cause global changes in the backbone dynamics on fast and slow time scales (72). This result may suggest that proteins are not always stabilized at a cost of conformational flexibility. Hydrogen-deuterium exchange studies can be applied to analyze the conformational flexibility of *T. thermophilus* RNase HI, because the backbone amide hydrogens of this protein have recently been assigned by using heteronuclear NMR spectroscopy (73). Therefore, it would be informative to analyze the conformational flexibility of the *T. thermophilus* RNase HI variant with enhanced catalytic efficiency and compare with that of the wild-type enzyme. These studies will facilitate the understanding for the relationships of stability, activity, and flexibility of enzymes in more detail.

2. 5 Conclusion

In this chapter, I showed that the Asp[134]→His mutation greatly reduced the catalytic activity of *T. thermophilus* RNase HI and the resultant mutant enzyme H[134]-TRNH could only poorly complement the ts phenotype of *E. coli* MIC3001. Random mutagenesis, followed by screening for second-site revertants, allowed me to isolate three single amino acid substitutions, Ala[12]→Ser, Lys[75]→Met, and Ala[77]→Pro, that increase the catalytic efficiency (k_{cat}/K_m) of *T. thermophilus* RNase HI. Combinations of these mutations cumulatively increased the catalytic efficiency of the enzyme without seriously affecting the stability. These results indicate that the activity of an enzyme from extreme thermophiles is not always inversely correlated with its stability.

Chapter 3. A DNA-linked RNase H with *T. thermophilus* RNase HI

Efficient Cleavage of RNA at High Temperatures by a Thermostable DNA-linked Ribonuclease H

3. 1 Introduction

In the previous chapters, I have analyzed the stability-activity-structure relationships of *T. thermophilus* RNase HI. In this chapter, I constructed a DNA-linked RNase H by crosslinking a DNA oligomer to *T. thermophilus* RNase HI, to examine this hybrid enzyme is more useful than that constructed using *E. coli* RNase HI for the site-specific cleavage of RNA at high temperatures.

It has previously been shown that the d9-$A^{13}A^{63}A^{133}C^{135}$-ERNH, in which the 9-mer DNA with a sequence of 5'-GTCATCTCC-3' is crosslinked to *E. coli* RNase HI, cleaves an RNA oligomer in a sequence-specific manner (Fig. 3-1) (19). The d9-$A^{13}A^{63}A^{133}C^{135}$-ERNH could also cleave 132- and 534-base RNAs, which were prepared by run-off transcription and contained a single target sequence, at the unique site within the target sequence (74). The usefulness of a DNA-linked RNase H for the cleavage of a specific mRNA has also been reported (75). In addition to DNA-linked RNase H, DNA-linked RNase A (76) and staphylococcal nuclease (77, 78) have been shown to cleave RNA site-specifically. However, DNA-linked RNase H has advantages over these DNA-linked enzymes in specificity and catalytic efficiency. DNA-linked RNase H cleaves the RNA only within the target sequence hybridized to the DNA adduct, which directs the RNase H portion to the RNA (Fig. 3-2). Moreover, the cleaved product of the RNA readily dissociates from the DNA adduct due to a reduced stability of RNA/DNA hybrid, and thereby the DNA-linked enzyme can perform multiple turnovers.

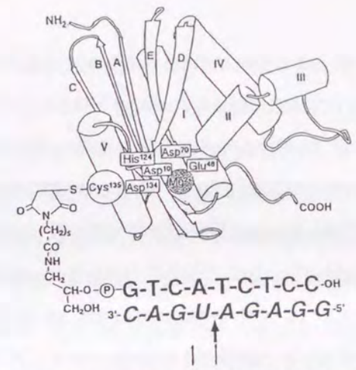

Fig. 3-1. Structure of the d9-$A^{13}A^{63}A^{133}C^{135}$-RNase H.
The d9-mer is covalently attached to Cys^{135}, which is substituted for Glu, through a linker. The r9-mer hybridized to the d9-mer portion of the d9-$A^{13}A^{63}A^{133}C^{135}$-RNase H, which is shown in an italic type, is cleaved at the site shown by a thick arrow. Cleavage sites of the r9-mer with the unmodified enzyme + d9-mer are shown by thin arrows.

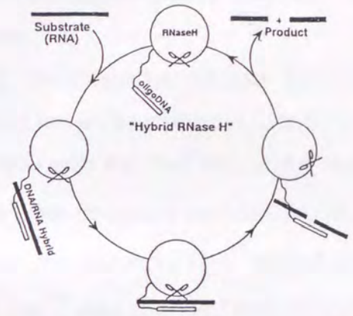

Fig. 3-2. A model for the mode of action of a DNA-linked RNase H.

The specificity and catalytic efficiency of DNA-linked RNase H have been shown to be affected by the size of the linker between the enzyme and DNA (79), and the size of DNA adduct (80). Of the various DNA-linked RNases H with different linkers in size, ranging from 18 to 27 Å, that with a 27 Å linker cleaved an oligomeric RNA substrate with the highest efficiency and site-selectivity. Likewise, of the various DNA-linked RNases H with different DNA adducts in size, ranging from 7-mer to 9-mer, that with an 8-mer DNA adduct most efficiently cleaved RNA site-specifically at 30 °C. In this case, the cleavage site was changed, such that the RNA substrate was cleaved at the site, which is located 5 residues downstream from the 5'-end of the RNA/DNA hybrid.

However, it remained to be determined whether a DNA-linked RNase H with altered function can be constructed by using RNases H from different sources, such as RNase HI from *T. thermophilus*, as a catalytic component of DNA-linked RNase H. Since *T. thermophilus* RNase HI is more stable than *E. coli* RNase HI by 33.9 °C in T_m (1), a DNA-linked RNase H with *T. thermophilus* RNase HI as a catalytic component (DNA-linked TRNH) may be useful to cleave RNA in a sequence-specific manner at high temperatures, at which a DNA-linked RNase H with *E. coli* RNase HI as a catalytic component (DNA-linked ERNH) will be thermally denatured.

3. 2 Experimental Procedures

Materials — The 15-mer RNA with a sequence of 5'-AAAAGAAAAGGGGGG-3' (PPT-RNA) was from Takara Shuzo Co., Ltd. The 15-mer DNA (5'-CCCCCCTTTTCTTTT-3') complementary to the PPT-RNA (d15-mer), and the d15-mer with aminohexyl (C_6) linker at the 5'-terminus (5'-amino-linked DNA) were synthesized by Vector Research Co., Ltd. N-(ε-maleimidecaproyloxy)succinimide was from Dojindo Laboratories. *Crotalus durissus* phosphodiesterase was from Boehringer Mannheim. The *E. coli* RNase HI variant, $A^{13}A^{63}A^{133}C^{135}$-ERNH, in which all cysteine residues (Cys^{13}, Cys^{63}, and Cys^{133}) were substituted by Ala and Glu^{135} was substituted by Cys, was prepared previously (19).

Preparation of T. thermophilus RNase HI mutants — Site-directed mutagenesis was carried out as described in Chapter 1 using a 5' - primer with the *Nde*I site, a 3' - primer with the *Sal*I site, and 5' and 3' mutagenic primers. The mutagenic primers were designed so that the codon for Cys^{13} was changed from TGC to TCG for Ser, the codon for Cys^{63} was changed from TGC to GCA for Ala, and the codon for Arg^{135} was changed from CGG to TGC for Cys. After the digestion by *Nde*I and *Sal*I, the PCR products were ligated to the *Nde*I-*Sal*I site of plasmid pJAL700T to construct expression vectors for the triple mutant enzyme $S^{13}A^{63}C^{135}$-TRNH with the $Cys^{13} \rightarrow$ Ser, $Cys^{63} \rightarrow$ Ala, and $Arg^{135} \rightarrow$ Cys mutations, the double mutant enzyme $A^{63}C^{135}$-TRNH with the $Cys^{63} \rightarrow$ Ala and $Arg^{135} \rightarrow$ Cys mutations, and the single mutant enzyme A^{63}-TRNH with the $Cys^{63} \rightarrow$ Ala mutation alone.

The overproducing strains were constructed by transforming *E. coli* HB101 with the resultant expression plasmids. Cultivation of the *E. coli* HB101 transformants with the plasmid pJAL700T derivatives, and overproduction and purification of the mutant enzymes were carried out as described in Chapter 1.

Construction of DNA-linked RNases H — The 5'-maleimide-d15-mer was

synthesized by the reaction between the 5'-amino-linked DNA and N-(ε-maleimidecaproyloxy)succinimide as previously described (19). Coupling reactions between the $S^{13}A^{63}C^{135}$-TRNH, the C^{13}-TRNH, or the $A^{13}A^{63}A^{133}C^{135}$-ERNH and the 5'-maleimide-d15-mer, and the purification of the resultant DNA-linked RNases H (d15-$S^{13}A^{63}C^{135}$-TRNH, d15-C^{13}-TRNH, or d15-$A^{13}A^{63}A^{133}C^{135}$-ERNH, respectively), were also carried out as previously described (19). These DNA-linked RNases H have a 27 Å linker [maleimide-$(CH_2)_5$-CONH-$(CH_2)_6$-].

Enzymatic activity — The RNase H activity was determined at 30 °C for 15 min in 20 µl of 10 mM Tris-HCl (pH 9.0) containing 1 mM $MgCl_2$ and 50 µg/ml acetylated bovine serum albumin (for *T. thermophilus* enzyme) or 10 mM Tris-HCl (pH 8.0), containing 10 mM $MgCl_2$, 50 mM NaCl, 1 mM 2-mercaptoethanol, and 50 µg/ml acetylated bovine serum albumin (for *E. coli* enzyme) by measuring the radioactivity of the acid-soluble digestion product from the substrate, ^{3}H-labeled M13 RNA/DNA hybrid, as previously described (29). One unit is defined as the amount of enzyme producing 1 µmol of acid-soluble material/min. The specific activity was defined as the enzymatic activity/mg of protein. The protein concentration was determined from the UV absorption at 280 nm, assuming that the mutant enzymes have the same $A_{280}^{0.1\%}$ values as those of the wild-type enzymes (1.6 for *T, thermophilus* RNase HI (1) and 2.02 for *E. coli* RNase HI (35)). The concentrations of the DNA-linked enzymes were also determined from the UV absorption at 280 nm assuming that the molar absorption coefficients of the d15-$S^{13}A^{63}C^{135}$-TRNH, d15-A^{63}-TRNH, and d15-$A^{13}A^{63}A^{133}C^{135}$-ERNH are 1.47×10^5, 1.47×10^5, and 1.53×10^5, respectively. These values are the sum of the molar absorption coefficients of the enzyme (2.9×10^4 for the *T. thermophilus* RNase HI derivatives and 3.5×10^4 for the *E. coli* RNase HI derivative) and the d15-mer (1.18×10^5).

Cleavage of oligonucleotide substrate — The PPT-RNA was ^{32}P-labeled at the 5'-end and was used as a substrate representing a single-strand RNA. This substrate (10 pmol) was hydrolyzed with the DNA-linked enzyme or the mixture of the unmodified enzyme and the unlinked d15-mer (molar ratio of 1:1) at various temperatures in 10 µl of the same buffer as for the digestion of M13 RNA/DNA hybrid. Prior to the reaction, the enzyme solution was incubated at each temperature for 15 min. The hydrolysates were separated on a 20 % polyacrylamide gel containing 7 M urea and were analyzed with Instant Imager (Packard). These hydrolysates were identified by comparing their migrations on the gel with those of the oligonucleotides generated by the partial digestion of the ^{32}P-labeled PPT-RNA with snake venom phosphodiesterase (81).

3. 3 Results and Discussion

Design of mutations — DNA-linked ERNH has been constructed by cross-linking a DNA oligomer to the cysteine residue substituted for Glu^{135} (19) based on the model for enzyme-substrate complex (49). The crystal structure of *T. thermophilus* RNase HI indicates that Arg^{135} is located at the equivalent position to Glu^{135} of *E. coli* RNase HI (Fig. 3-3). Therefore, I decided to substitute Cys for this arginine residue. In order to crosslink a DNA oligomer specifically to the thiol group at position 135, other free thiol groups should be eliminated. In fact, for the construction of DNA-linked ERNH, all three cysteine residues with free thiol groups were replaced by Ala to make the thiol group of Cys^{135} unique. *T. thermophilus* RNase HI contains four cysteine residues at positions 13, 41, 63, and 149. The localizations of these cysteine residues, except for that of Cys^{149}, in the crystal structure of *T. thermophilus* RNase HI are shown in Fig. 3-3. However, it seems desirable to leave Cys^{41} and Cys^{149} unchanged, because these residues contribute to the protein stability by spontaneously forming a disulfide bond between them in the absence of a reducing reagent (Chapter 1). In addition, it has previously been shown for the *T. thermophilus* RNase HI variant, which lacks the C-terminal 12 residues, that the $Cys^{63} \rightarrow$ Ala mutation does not seriously affect the enzymatic activity, whereas the $Cys^{13} \rightarrow$ Ala mutation greatly reduces it (Chapter 1). Therefore, I decided to replace Cys^{13} and Cys^{63} with Ser and Ala, respectively. The $Cys^{13} \rightarrow$ Ser mutation is expected to affect the enzymatic activity less seriously than the $Cys^{13} \rightarrow$ Ala mutation, because the former is more conservative than the latter. In addition to the resultant triple mutant enzyme $S^{13}A^{63}C^{135}$-TRNH, the double and single mutant enzymes $A^{63}C^{135}$-TRNH and A^{63}-TRNH were constructed to analyze the effect of the individual mutations on the enzymatic activity.

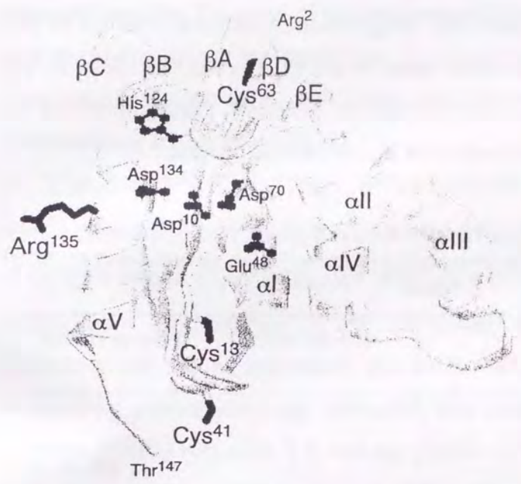

Fig. 3-3. Three-dimensional structure of *T. thermophilus* RNase HI.
The backbone structure of *T. thermophilus* RNase HI, determined by Ishikawa *et al.* (27), was drawn with the program RasMol. Arg^{2} and Thr^{147} represent the N- and C-terminal residues in this crystal structure, because the N-terminal region from Met^{-4} to Pro^{1} and the C-terminal region from Pro^{148} to Ala^{161} have not been defined by crystallographic analyses, probably due to structural disorder. The side chains of Cys^{13}, Cys^{41}, Cys^{63}, and Arg^{135}, as well as those of the active-site residues (Asp^{10}, Glu^{48}, Asp^{70}, His^{124}, and Asp^{134}), are indicated. This crystal structure of *T. thermophilus* RNase HI has been deposited in the Brookhaven Protein Data Bank under accession number 1RIL.

Activities of the mutant enzymes — The activities of the wild-type and mutant enzymes of *T. thermophilus* RNase HI for the hydrolysis of the M13 RNA/DNA hybrid are summarized in Table 3-1, in comparison with those of *E. coli* RNase HI. The $Cys^{63} \rightarrow$ Ala mutation did not seriously affect the enzymatic activity of *T. thermophilus* RNase HI as expected. Comparison of the specific activities of the A^{63}-TRNH and $A^{63}C^{135}$-TRNH indicates that the $Arg^{135} \rightarrow$ Cys mutation reduced the enzymatic activity of the A^{63}-TRNH by 53 %. Likewise, comparison of the specific activities of the $A^{63}C^{135}$-TRNH and $S^{13}A^{63}C^{135}$-TRNH indicates that the $Cys^{13} \rightarrow$ Ser mutation reduced the enzymatic activity of the $A^{63}C^{135}$-TRNH by 84 %. Because the $Cys^{13} \rightarrow$ Ala mutation has been reported to reduce the enzymatic activity of *T. thermophilus* RNase HI by 83% (Table 1-2), the $Cys^{13} \rightarrow$ Ser and $Cys^{13} \rightarrow$ Ala mutations reduced the enzymatic activity of *T.*

thermophilus RNase HI by a similar extent. Mutational and structural studies of *E. coli* RNase HI have suggested that Cys^{13} is engaged in substrate binding through the formation of a hydrogen bond between the main chain carbonyl oxygen of Cys^{13} and the substrate (49). Slight conformational change of this oxygen atom caused by the mutation may result in a great reduction in the enzymatic activity of *T. thermophilus* RNase HI. However, these mutations do not seriously affect the catalytic function of *E. coli* RNase HI (35).

Table 3-1
Specific activities of the mutant and DNA-linked enzymes for the hydrolysis of the M13 RNA/DNA hybrid

Enzyme	Mutation	Specific activity[a] (units/mg)	Relative activity[b] (%)
WT-TRNH	-	1.6	100
A^{63}-TRNH	$C^{63}\rightarrow A$	1.5	94
d15-A^{63}-TRNH		0.011	0.69 (0.73)
$A^{63}C^{135}$-TRNH	$C^{63}\rightarrow A$, $R^{135}\rightarrow C$	0.70	44
$S^{13}A^{63}C^{135}$-TRNH	$C^{13}\rightarrow S$, $C^{63}\rightarrow A$, $R^{135}\rightarrow C$	0.11	6.9
d15-$S^{13}A^{63}C^{135}$-TRNH		0.011	0.69 (10)
WT-ERNH	-	14.3	100
$A^{13}A^{63}A^{133}C^{135}$-ERNH	$C^{13}\rightarrow A$, $C^{63}\rightarrow A$, $C^{133}\rightarrow A$, $E^{135}\rightarrow C$	5.3	37
d15-$A^{13}A^{63}A^{133}C^{135}$-ERNH		0.60	4.2 (11)

[a]Errors are the same as those described in the legend for Table 1-1.
[b]The relative activity was calculated by dividing the specific activity of the mutant or DNA-linked enzyme by that of the corresponding wild-type enzyme. The relative activity (%) of each DNA-linked enzyme to that of its parent mutant enzyme was shown in parenthesis.

Construction of DNA-linked RNases H — Because DNA-linked RNase H cleaves the RNA substrate when its DNA adduct forms a RNA/DNA hybrid with the substrate, any DNA oligomer can be linked to RNase H. In this study, I chose the d15-mer, which is complementary to the PPT sequence of HIV-1 RNA, as a DNA adduct. This PPT sequence is not degraded by the RNase H activity of reverse transcriptase (RT) during the synthesis of the minus-strand DNA and serves as a primer for the synthesis of the plus-strand DNA (82). The DNA-linked RNase H with a nonadeoxyribonucleotide (d9-mer) adduct was previously constructed (19). However, DNA-linked RNases H with the d15-mer

adduct is more suitable than those with the d9-mer adduct to compare the activities of DNA-linked ERNH and TRNH, because the 15-bp RNA/DNA hybrid must be more stable than the 9-bp RNA/DNA hybrid. Itakura *et al.* (83) have reported that the T_m value of the oligomeric DNA/DNA duplex increases as its size and GC content increase. The T_m value of the d9-mer/r9-mer hybrid has been reported to be 49 °C (19), indicating that this substrate is not stable at the temperatures higher than 50 °C.

The d15-$S^{13}A^{63}C^{135}$-TRNH, d15-A^{63}-TRNH, and d15-$A^{13}A^{63}A^{133}C^{135}$-ERNH were constructed by linking the d15-mer through a 27 Å linker to Cys^{135} of the $S^{13}A^{63}C^{135}$-TRNH, Cys^{13} of the A^{63}-TRH, and Cys^{135} of the $A^{13}A^{63}A^{133}C^{135}$-ERNH, respectively. Comparison of the enzymatic activities of these DNA-linked RNases H for the hydrolysis of the M13 RNA/DNA hybrid with those of the unmodified parent enzymes indicated that crosslinking of the d15-mer to the enzyme greatly reduced the activity (Table 3-1), probably because the DNA adduct interferes with the binding of the RNA/DNA substrate to the enzyme. However, the enzymatic activities of the d15-$S^{13}A^{63}C^{135}$-TRNH and d15-$A^{13}A^{63}A^{133}C^{135}$-ERNH were ~10% of those of the unmodified parent enzymes, whereas the enzymatic activity of the d15- A^{63}-TRNH was 0.7 % of that of the A^{63}-TRNH. The inhibitory effect of the DNA adduct linked to Cys^{13} is much larger than that linked to Cys^{135}, probably because Cys^{13} is located more closely to the substrate binding site. A large cleft-like depression, which extends from the negatively charged active-site formed by Asp^{10}, Glu^{48}, Asp^{70}, His^{124}, and Asp^{134} to the positively charged αIII-helix and the following loop (Fig. 3-3), has been proposed to form a substrate binding site of the enzyme (49).

Stability — The stability of the d15-$S^{13}A^{63}C^{135}$-TRNH against irreversible heat inactivation was compared with that of the d15-$A^{13}A^{63}A^{133}C^{135}$-ERNH by measuring the residual activities of these enzymes after heating at various temperatures for 15 min, in 10 mM Tris-HCl (pH 7.5) containing 0.1 M NaCl, 1 mM EDTA, 10 % glycerol, and 0.1 mg/ml of bovine serum albumin (Fig. 3-4). The residual activity was determined at 30 °C by using the PPT-RNA as a substrate. The d15-$S^{13}A^{63}C^{135}$-TRNH almost fully retained its activity after heating at 90 °C. In contrast, the d15-$A^{13}A^{63}A^{133}C^{135}$-ERNH lost 50 % of its activity after heating at 50 °C and was almost fully inactivated after heating at 60 °C. These results indicate that the d15-$S^{13}A^{63}C^{135}$-TRNH is much more stable than the d15-$A^{13}A^{63}A^{133}C^{135}$-ERNH.

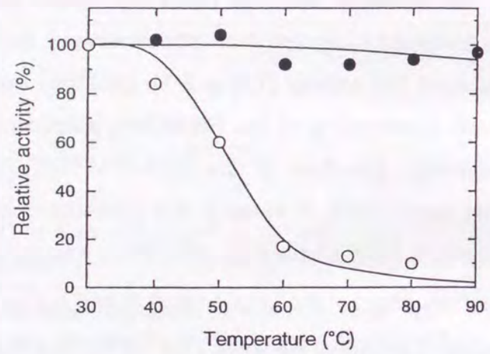

Fig. 3-4. Stability against irreversible heat inactivation.
The d15-$S^{13}A^{63}C^{135}$-TRNH (*closed circle*) and d15-$A^{13}A^{63}A^{133}C^{135}$-ERNH (*open circle*) were incubated for 15 min at the temperatures indicated, in 10 mM Tris-HCl (pH 7.5) containing 0.1 M NaCl, 1 mM EDTA, 10 % glycerol, and 0.1 mg/ml bovine serum albumin and determined for the residual activities by using PPT-RNA as a substrate at 30 °C. The concentrations of these enzymes were 0.16 μg/ml.

Cleavage of PPT-RNA — To examine whether and how the d15-$S^{13}A^{63}C^{135}$-TRNH, d15- A^{63}-TRNH, and d15-$A^{13}A^{63}A^{133}C^{135}$-ERNH cleave the single-stranded RNA, the 15-base PPT-RNA labeled at its 5'-end was used as a substrate. The cleavage of this substrate with the mixture of the unmodified parent enzyme and the unlinked d15-mer (molar ratio of 1:1) was also

examined for the comparative purpose. The results obtained at 65°C were shown in Fig. 3-5A and summarized in Fig. 3-5B, as representatives.

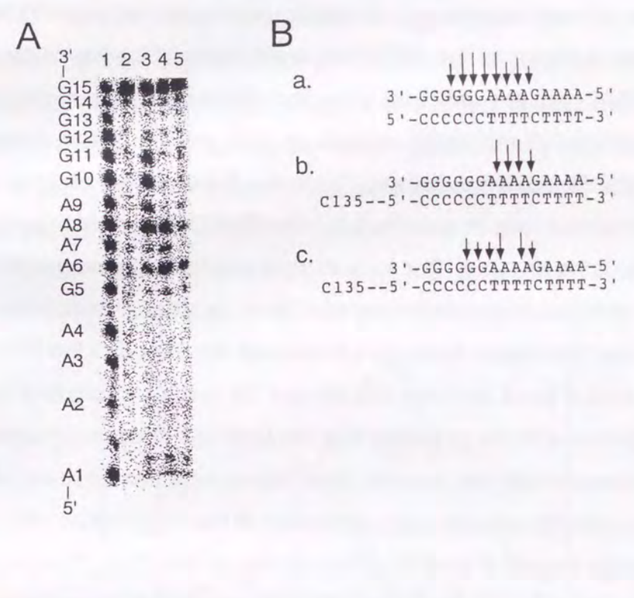

Fig. 3-5. Cleavage of the PPT-RNA by the DNA-linked enzymes.
(A) Autoradiograph of cleavage reactions. The hydrolyses of the 5' end-labeled PPT-RNA (10 pmol) with the DNA-linked enzymes or the mixture of the unmodified enzyme and the d15-mer were carried out at 65 °C for 15 min and the hydrolysates were separated on a 20 % polyacrylamide gel containing 7 M urea as described under Materials and methods. The concentration of the substrate is 1.0 μM. Lane 1, partial digest of the PPT-RNA with snake venom phosphodiesterase; lane 2, untreated PPT-RNA; lane 3, hydrolysate of the PPT-RNA with the mixture of 3.1 ng (0.16 pmol) of the $S^{13}A^{63}C^{135}$-TRNH and 0.16 pmol of the d15-mer DNA; lane 4, hydrolysate of the PPT-RNA with 0.078 ng (0.004 pmol) of the d15-$S^{13}A^{63}C^{135}$-TRNH; lane 5; hydrolysate of the PPT-RNA with 16 ng (0.8 pmol) of the d15-A^{63}-TRNH. (B) The sites and extents of cleavages by the DNA-linked and unlinked enzymes. Cleavage sites of the PPT-RNA with the mixture of the $S^{13}A^{63}C^{135}$-TRNH and d15-mer (a), with the d15-$S^{13}A^{63}C^{135}$-TRNH (b), and with the d15-A^{63}-TRNH (c) are shown by *arrows*. Difference in the size of *arrows* reflects the relative cleavage intensities at the indicated position. The cleavage sites of this substrate with $A^{13}A^{63}A^{133}C^{135}$-ERNH and d15-$A^{13}A^{63}A^{133}C^{135}$-ERNH were almost identical with those with $S^{13}A^{63}C^{135}$-TRNH and d15-$S^{13}A^{63}C^{135}$-TRNH, respectively. The upper and lower sequences represent RNA and DNA, respectively. The positions of the $S^{13}A^{63}C^{135}$-TRNH are indicated for the RNA/DNA hybrids formed between the PPT-RNA and the d15-mer linked to the enzyme.

The d15-S^{13}A^{63}C^{135}-TRNH cleaved the PPT-RNA preferably at two positions, A6-A7 and A8-A9, and less preferably at two positions, G5-A6 and A7-A8. Thus, four phosphodiester bonds located between G5 and A9 of the PPT-RNA are susceptible to the cleavage with the d15-S^{13}A^{63}C^{135}-TRNH. In contrast, additional four phosphodiester bonds, which are located between A9 and G13 at the 3'-terminal region of the PPT-RNA, were cleaved by the mixture of the S^{13}A^{63}C^{135}-TRNH and the unlinked d15-mer. These results suggest that the crosslinking of the d15-mer to the enzyme restricts the interaction between the enzyme and the RNA/DNA substrate. The linker between the enzyme and the d15-mer must form a loop in order to bring the RNA/DNA hybrid in contact with the active-site of the enzyme. This loop might prevent the cleavage of the PPT-RNA at its 3'-terminal region, because of a steric constraint. In addition, Fig. 3-5B indicates that the major cleavage site nearest the 5'-end of the PPT-RNA is the phosphodiester bond between the 6th and 7th residues from its 5'-end. This result is consistent with the proposal that the DNA residues complementary to the RNA residues, which are located six or seven residues upstream from the cleavage site, interact with the basic protrusion of the enzyme (84, 85).

The cleavage modes of the PPT-RNA with the d15-S^{13}A^{63}C^{135}-TRNH and the mixture of the S^{13}A^{63}C^{135}-TRNH and d15-mer at different temperatures, and those with the d15-A^{13}A^{63}A^{133}C^{135}-ERNH and the mixture of the A^{13}A^{63}A^{133}C^{135}-ERNH and d15-mer at the temperatures lower than 50 °C were basically identical with those shown in Fig. 3-5. However, the d15-A^{63}-TRNH cleaved the PPT-RNA as did the mixture of the A^{63}-TRNH and the unlinked d15-mer, but with a greatly reduced efficiency (Fig. 3-5A), suggesting that this DNA-linked enzyme cannot cleave the PPT-RNA hybridized to its DNA adduct in an unimolecular fashion, but cleaves the PPT-RNA hybridized to the DNA adduct of another d15-A^{63}-TRNA molecule in a bimolecular fashion.

The d15-S^{13}A^{63}C^{135}-TRNH and d15-A^{13}A^{63}A^{133}C^{135}-ERNH showed the highest specific activities for the hydrolysis of the PPT-RNA at 65 °C and 50 °C, respectively (Fig. 3-6). The former was 1.8 fold higher than the latter. As a result, the d15-S^{13}A^{63}C^{135}-TRNH cleaves the PPT-RNA more effectively than the d15-A^{13}A^{63}A^{133}C^{135}-ERNH at the temperatures higher than 50 °C. The optimum temperature of the d15-A^{13}A^{63}A^{133}C^{135}-ERNH is clearly governed by the thermostability of the DNA-linked enzyme. In contrast, the optimum temperature of the d15-S^{13}A^{63}C^{135}-TRNH seems to be governed by the stability of the enzyme-linked RNA/DNA hybrid, because the d15-S^{13}A^{63}C^{135}-TRNH is highly stable as shown in Fig. 3-4.

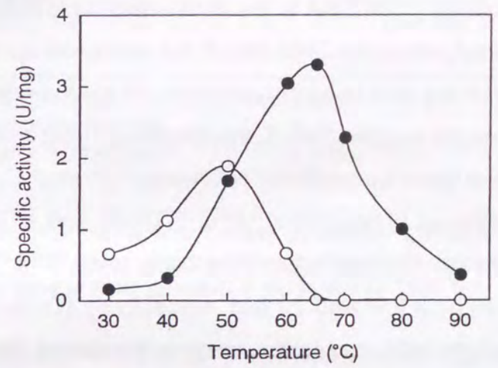

Fig. 3-6. Optimum temperatures of the DNA-linked enzymes.
The enzymatic activities of the d15-S^{13}A^{63}C^{135}-TRNH (*solid circle*) and d15-A^{13}A^{63}A^{133}C^{135}-ERNH (*open circle*) for the hydrolysis of the PPT-RNA were determined for 15 min at the temperatures indicated, in 10 mM Tris-HCl (pH 9.0) containing 1 mM $MgCl_2$ and 50 μg/ml acetylated bovine serum albumin (for d15-S^{13}A^{63}C^{135}-TRNH) or in 10 mM Tris-HCl (pH 8.0) containing 10 mM $MgCl_2$, 50 mM NaCl, 1 mM 2-mercaptoethanol, and 50 μg/ml acetylated bovine serum albumin (for d15-A^{13}A^{63}A^{133}C^{135}-ERNH). Prior to the reaction, the enzyme solution was incubated at each temperature for 15 min.

The specific activities of the DNA-linked enzymes and unmodified parent enzymes determined by using the PPT-RNA as a substrate at 30 °C and 65 °C are summarized in Table 3-2. The specific activities of the unmodified enzymes represent those determined for the mixture of the unmodified enzyme and the unlinked d15-mer (molar ratio of 1:1). The specific activity of the $S^{13}A^{63}C^{135}$-TRNH (0.016 u/mg) was 48 % of that of the $A^{13}A^{63}A^{133}C^{135}$-ERNH (0.033 u/mg) at 30 °C (Table 3-2). This result is inconsistent with that obtained by the M13 RNA/DNA hybrid as a substrate, which shows that the specific activity of the $S^{13}A^{63}C^{135}$-TRNH (0.11 u/mg) is 2.1 % of that of the $A^{13}A^{63}A^{133}C^{135}$-ERNH (5.3 u/mg) at 30 °C (Table 3-1). When the PPT-RNA was used as a substrate, a large excess amount of the RNA substrate is present over DNA, and a multiple turnover of hybridization of the DNA to the RNA substrate is required for efficient hydrolysis. In contrast, when the M13 RNA/DNA was used as a substrate, the hybrid is already formed and is hydrolyzed without the hybridization process. Therefore, these results suggest that *T. thermophilus* RNase HI possesses an ability to promote the formation of RNA/DNA hybrid.

The specific activities of the d15-$S^{13}A^{63}C^{135}$-TRNH and d15-$A^{13}A^{63}A^{133}C^{135}$-ERNH determined at 30 °C were higher than those of the $S^{13}A^{63}C^{135}$-TRNH and $A^{13}A^{63}A^{133}C^{135}$-ERNH by 8 fold and 20 fold, respectively (Table 3-2), indicating that crosslinking of the d15-mer to the enzyme increased the activity of the enzyme. Because the d15-mer was crosslinked to the enzyme such that the PPT-RNA hybridized to this d15-mer is positioned in a close proximity to the substrate-binding and active-site of the enzyme, these DNA-linked enzymes would immediately cleave the PPT-RNA once it formed a RNA/DNA hybrid. This enhancement of the enzymatic activity by the crosslinking became more remarkable at 65 °C for the $S^{13}A^{63}C^{135}$-TRNH, because the activity of the d15-$S^{13}A^{63}C^{135}$-TRNH was increased by 25 fold at 65 °C, whereas that of the $S^{13}A^{63}C^{135}$-TRNH was unchanged at 65 °C. As a result, the specific activity of the d15-$S^{13}A^{63}C^{135}$-TRNH was higher than that of the $S^{13}A^{63}C^{135}$-TRNH by 210 fold at 65 °C. It has previously been reported that the specific activity of *T. thermophilus* RNase HI for the hydrolysis of the M13 RNA/DNA hybrid

determined at 70 °C was 14-fold higher than that determined at 37 °C. Therefore, the specific activity of the $S^{13}A^{63}C^{135}$-TRNH was unchanged at 65 °C, probably because the d15-mer may not form a stable hybrid with the PPT-RNA at 65 °C. Alternatively, a large excess amount of the PPT-RNA over DNA may inhibit the activity of the $S^{13}A^{63}C^{135}$-TRNH more seriously at 65 °C than at 30 °C. Unlike the crosslinking of the $S^{13}A^{63}C^{135}$-TRNH or $A^{13}A^{63}A^{133}C^{135}$-ERNH, that of the A^{63}-TRNH greatly reduced its activity (data not shown), indicating that Cys^{13} is not a suitable for crosslinking.

Table 3-2

Specific activities of the DNA-linked and unlinked enzymes for the hydrolysis of the PPT-RNA at different temperatures

Enzyme	Specific activity[a] (units/mg)	
	30 ℃	65 ℃
$S^{13}A^{63}C^{135}$-TRNH	0.016	0.016
d15-$S^{13}A^{63}C^{135}$-TRNH	0.13	3.3
$A^{13}A^{63}A^{133}C^{135}$-ERNH	0.033	<0.01
d15-$A^{13}A^{63}A^{133}C^{135}$-ERNH	0.66	<0.01

[a]The specific activity of the $S^{13}A^{63}C^{135}$-TRNH or $A^{13}A^{63}A^{133}C^{135}$-ERNH was determined by hydrolyzing the PPT-RNA by the mixture of this enzyme and the unlinked d15-mer (molar ratio of 1:1). Errors are the same as those described in the legend for Table 1-1.

It is noted that the PPT-RNA/d15-mer hybrid, which must not be cleaved by the RNase H activity of HIV-1 RT, is cleaved by *E. coli* or *T. thermophilus* RNase HI. It has been proposed that RNases H recognize a RNA/DNA hybrid as a substrate because it assumes an H-form structure (86). The minor groove width in the H-form structure is larger and smaller than those in the B-form and A-form structures, respectively (86). However, structural studies have recently shown that a PPT-RNA/DNA hybrid assumes an A-form, instead of an H-form, structure (87, 88). This may be the reason why the RNase H activity of HIV-1 RT cannot cleave a PPT-RNA/DNA hybrid. However, it remained to be determined whether a PPT-RNA/DNA hybrid assumes an H-form structure upon binding to *E. coli* or *T. thermophilus* RNase HI, or these RNases H recognize the structure of a RNA/DNA hybrid in a less strict manner.

3. 4 Conclusion

In this chapter, I constructed the d15-S^{13}A^{63}C^{135}-TRNH and d15-A^{13}A^{63}A^{133}C^{135}-ERNH, in which the 15-mer DNA with a sequence complementary to the polypurine-tract (PPT) sequence of HIV-1 RNA is attached through a 27 Å linker to Cys^{135} of the *T. thermophilus* and *E. coli* RNases HI mutants. I showed that the d15-S^{13}A^{63}C^{135}-TRNH cleaved the 15-mer RNA with the PPT sequence more effectively than the d15-A^{13}A^{63}A^{133}C^{135}-ERNH at the temperatures higher than 50 °C. Therefore, DNA-linked TRNH may be useful for the cleavage of RNA molecules at high temperatures, at which highly ordered structures of RNA molecules will be thermally denatured.

General Conclusion

In this thesis, I focused on the stability and activity of *T. thermophilus* RNase HI to get more information on the stability-activity-structure relationships of this enzyme.

In chapter 1, to identify factors that contribute to the thermal stability of *T. thermophilus* RNase HI, protein variants with a series of carboxyl-terminal truncations and Cys → Ala mutations were constructed, and their thermal denaturations were analyzed by CD. The results indicate that Cys^{41} and Cys^{149} contribute to the protein stability, probably through the formation of a disulfide bond. Peptide mapping analysis for the mutant protein with only two cysteine residues, at positions 41 and 149, indicated that this disulfide bond was partially formed in a protein purified from *E. coli* in the absence of a reducing reagent but was fully formed in a thermally denatured protein. These results suggest that the thermal stability of *T. thermophilus* RNase HI, determined in the absence of a reducing reagent, reflects that of an oxidized form of the protein. Comparison of the thermal stabilities and the enzymatic activities of the wild-type and truncated proteins, determined in the presence and absence of a reducing reagent, indicates that the formation of this disulfide bond increases the thermal stability of the protein by 6-7 °C in T_m and approximately 3 kcal/mol in ΔG_m without seriously affecting the enzymatic activity. Since *T. thermophilus* RNase HI is present in a reducing environment in cells, this disulfide bond probably is not formed in vivo but is spontaneously formed in vitro in the absence of a reducing reagent. Therefore, the difference in the in vivo stability between *T. thermophilus* and *E. coli* RNase HI must be ~25 °C in T_m.

In chapter 2, a genetic method to isolate a mutant enzyme of *T. thermophilus* RNase HI with enhanced activity at moderate temperatures was developed. *T. thermophilus* RNase HI has an ability to complement the RNase H-dependent temperature-sensitive (ts) growth phenotype of *E. coli* MIC3001. However, this complementation ability was greatly reduced by replacing Asp^{134}, which is one of the active-site residues, with His, probably due to a reduction in the catalytic

activity. Random mutagenesis of the gene encoding the resultant D134H enzyme, followed by screening for second-site revertants, allowed me to isolate three single mutations (Ala^{12}→Ser, Lys^{75}→Met, and Ala^{77}→Pro) that restore the normal complementation ability to the D134H enzyme. These mutations were individually or simultaneously introduced into the wild-type enzyme and the kinetic parameters of the resultant mutant enzymes for the hydrolysis of a DNA-RNA-DNA/DNA substrate were determined at 30 °C. Each mutation increased the k_{cat}/K_m value of the wild-type enzyme by 2.1-4.8 fold. The effects of the mutations on the enzymatic activity were roughly cumulative and the combination of these three mutations increased the k_{cat}/K_m value of the wild-type enzyme by 40 fold (5.5 fold in k_{cat}). Measurement of thermal stability of the mutant enzymes with CD in the presence of 1 M GdnHCl and 1 mM DTT showed that the T_m value of the triple mutant enzyme, in which all three mutations were combined, was comparable to that of the wild-type enzyme (75.0 °C vs. 77.4 °C). These results demonstrate that the activity of a thermophilic enzyme can be improved without a cost of protein stability.

In chapter 3, to construct a DNA-linked RNase H, which cleaves RNA site-specifically at high temperatures, the 15-mer DNA, which is complementary to the polypurine-tract sequence of human immunodeficiency virus-1 RNA (PPT-RNA), was crosslinked to the unique thiol group of Cys^{135} in the *T. thermophilus* RNase HI variant. The resultant DNA-linked enzyme (d15-$S^{13}A^{63}C^{135}$-TRNH), as well as the d15-$A^{13}A^{63}A^{133}C^{135}$-ERNH, in which the RNase H portion of the d15-$S^{13}A^{63}C^{135}$-TRNH is replaced by the *E. coli* RNase HI variant, cleaved the 15-mer PPT-RNA site-specifically. The mixture of the unmodified enzyme and the unlinked 15-mer DNA also cleaved the PPT-RNA but in a less strict manner. In addition, this mixture cleaved the PPT-RNA much less effectively than the DNA-linked enzyme. These results indicate that the crosslinking limits but accelerates the interaction between the enzyme and the RNA/DNA substrate. The d15-$S^{13}A^{63}C^{135}$-TRNH cleaved the PPT-RNA more effectively than the d15-$A^{13}A^{63}A^{133}C^{135}$-ERNH at the temperatures higher than 50 °C. The d15-$S^{13}A^{63}C^{135}$-TRNH showed the highest activity at 65 °C, at which the d15-

$A^{13}A^{63}A^{133}C^{135}$-ERNH showed little activity. Therefore, DNA-linked TRNH may be useful for the cleavage of RNA molecules with highly ordered structures. DNA-linked ERNH cannot cleave these RNA molecules, because its DNA adduct cannot hybridize to the target sequence. Thermal denaturation and renaturation of these RNA molecules in the presence of DNA-linked TRNH may facilitate this hybridization and thereby facilitate the sequence-specific cleavage of these RNA molecules, because DNA-linked TRNH will not be denatured at these temperatures.

From these results, following conclusions were drawn.

1. It has been suggested that a decrease in cysteine residues contributes to the thermostability of enzymes from thermophilic bacteria (34), because a spontaneous formation of a non-natural disulfide bond of which formation is accelerated at high temperatures, is often unfavorable for the thermostability of a thermophilic enzyme. However, *T. thermophilus* RNase HI is effectively stabilized by the spontaneous formation of the disulfide bond. Thus, the spontaneous formation of the disulfide bond does not always destabilize a thermophilic enzyme.
2. The thermostability of *T. thermophilus* RNase HI can be improved without a cost of the enzymatic activity by the introduction of a disulfide bond. Likewise, the enzymatic activity of this enzyme at moderate temperatures can be improved without a cost of the thermostability by in vitro evolution method. Thus, the activity and stability of a thermophilic enzyme is not always inversely correlated with each other, as well as those of a mesophilic enzyme.
3. The oxidized form of *T. thermophilus* RNase HI, which is stabilized by 6-7 °C in T_m, or the triple mutant enzyme, which is activated by 40 fold in k_{cat}/K_m, may be more useful than the reduced form or the wild-type enzyme, as a tool for recombinant DNA and RNA technologies. In fact, DNA-linked enzyme constructed using the oxidized form of *T. thermophilus* RNase HI was shown to be useful as an artificial RNA restriction enzyme at high temperatures.

References

1. Kanaya, S., and Itaya, M. (1992) *J. Biol. Chem. 267*, 10184-10192.
2. Wrba, A., Schweiger, A., Schultes, V., and Jaenicke, R. (1990) *Biochemistry* **29**, 7584-7592.
3. Varley, P. G., and Pain, R. H. (1991) *J. Mol. Biol.* **220**, 531-538.
4. Zavodszky, P., Kardos, J., Svingor, A., and Petsko, G. A. (1998) *Proc. Natl. Acad. Sci. U.S.A.* **95**, 7406-7411.
5. Kohen, A., Cannio, R., Bartolucci, S., and Klinman, J. P. (1999) *Nature* **399**, 496-499.
6. Meiering, E. M., Serrano, L., and Fersht, A. R. (1992) *J. Mol. Biol.* **225**, 585-589.
7. Shoichet, B. K., Baase, W. A., Kuroki, R., and Matthews, B. W. (1995) *Proc. Natl. Acad. Sci. U.S.A.* **92**, 452-456.
8. Kidokoro, S., Miki, Y., Endo, K., Wada, A., Nagao, H., Miyake, T., Aoyama, A., Yoneya, T., Kai, K., and Ooe, S. (1995) *FEBS Lett.* **367**, 73-76.
9. Kimura, S., Nakamura, H., Hashimoto, T., Oobatake, M. and Kanaya, S. (1992) *J. Biol. Chem.* **267,** 21535-21542.
10. Kimura, S., Kanaya, S. and Nakamura, H. (1992) *J. Biol. Chem.* **267,** 22014-22017.
11. Ishikawa, K., Nakamura, H., Morikawa, K. and Kanaya, S. (1993) *Biochemistry* **32,** 6171-6178.
12. Akasako, A., Haruki, M., Oobatake, M., and Kanaya, S. (1995) *Biochemistry* **34**, 8115-8122.
13. Giver, L., Gershenson, A., Freskgard, P. O., and Arnold, F. H. (1998) *Proc. Natl. Acad. Sci. U.S.A.* **95**, 12809-12813.
14. Chen, K., and Arnold, F. H. (1993) *Proc. Natl. Acad. Sci. U.S.A.* **90**, 5618-5622.
15. Wan, L., Twitchett, M. B., Eltis, L. D., Mauk, A. G., and Smith, M. (1998) *Proc. Natl. Acad. Sci. U.S.A.* **95**, 12825-12831.
16. Zhao, H., and Arnold, F. H. (1999) *Protein Eng.* **12**, 47-53.

17. Matsuura, T., Miyai, K., Trakulnaleamsai, S., Yomo, T., Shima, Y., Miki, S., Yamamoto, K., and Urabe, I. (1999) *Nat. Biotechnol.* **17**, 58-61.
18. Crouch, R. J., and Dirksen, M. -L. (1982) in *Nuclease* (Linn, S. M., & Roberts, R. J., eds) pp. 211-241, Cold Spring Harbor Laboratory, Cold Spring Harbor, NY
19. Kanaya,S., Nakai,C., Konishi,A., Inoue,H., Ohtsuka,E. and Ikehara,M. (1992) *J. Biol. Chem.*, **267**, 8492-8498.
20. Kanaya, S., and Crouch, R. J. (1983) *J. Biol. Chem. 258*, 1276-1281
21. Ohtani, N., Haruki, M., Morikawa, M., and Kanaya, S. (1999) *J. Biosci. Bioeng. 88*, 12-19.
22. Crouch, R. J. (1990) *New Biol. 2*, 771-777.
23. Hostomsky, Z., Hostomska, Z., and Matthews, D. A. (1993) in *Nucleases, 2nd edition* (Linn, S. M., and Roberts, R. J., Eds.) pp.341-376, Cold Spring Harbor Laboratory, Cold Spring Harbor, NY
24. Kanaya, S. (1998) in *Ribonucleases H* (Crouch, R. J., and Toulme, J. J., Eds.) pp. 1-38, INSERM, Paris.
25. Katayanagi, K., Miyagawa, M., Matsushima, M., Ishikawa, M., Kanaya, S., Ikehara, M., Matsuzaki, T. and Morikawa, K. (1990) *Nature* **347**, 306-309.
26. Katayanagi, K., Miyagawa, M., Matsushima, M., Ishikawa, M., Kanaya, S., Nakamura, H., Ikehara, M., Matsuzaki, T. and Morikawa, K. (1992) *J. Mol. Biol.* **223**, 1029-1052.
27. Yang, W., Hendrickson, W. A., Crouch, R. J. and Satow, Y. (1990) *Science* **249**, 1398-1405.
28. Ishikawa, K., Okumura, M., Katayanagi, K., Kimura, S., Kanaya, S., Nakamura, H. and Morikawa, K. (1993) *J. Mol. Biol.* **230,** 529-542.
29. Kanaya, S., Katsuda, C., Kimura, S., Nakai, T., Kitakuni, E., Nakamura, H., Katayanagi, K., Morikawa, K. and Ikehara, M. (1991) *J. Biol. Chem.* **266,** 6038-6044.
30. Haruki, M., Noguchi, E., Akasako, A., Oobatake, M., Itaya, M. and Kanaya, S. (1994) *J. Biol. Chem.* **269,** 26904-26911.
31. Ishikawa, K., Kimura, S., Kanaya, S., Morikawa, K., and Nakamura, H.

(1993) *Protein Engineering* **6**, 85-91.
32. Saito, M., and Tanimura, R. (1995) *Chem. Phys. Lett.* **236**, 156-161.
33. Tanimura, R., and Saito, M. (1996) *Mol. Simul.* **16**, 75-85.
34. Koyama, Y., and Furukawa, K. (1990) *J. Bacteriol.* **172**, 3490-3495.
35. Kanaya, S., Kimura, S., Katsuda, C., and Ikehara, M. (1990) *Biochem. J.* **271**, 59-66.
36. Watanabe, K., Chishiro, K., Kitamura, K., and Suzuki, Y. (1991) *J. Biol. Chem.* **266**, 24287-24294.
37. Matthews, B. W., Nicholson, H., and Becktel, W. J. (1987) *Proc. Natl. Acad. Sci. USA* **84**, 6663-6667.
38. Kanaya, S., Oobatake, M., Nakamura, H., and Ikehara, M. (1993) *J. Biotechnol.* **28**, 117-136.
39. Sanger, F., Nicklen, S. and Coulson, A. R. (1977) *Proc. Natl. Acad. Sci. USA* **74**, 5463-5467.
40. Laemmli, U. K. (1970) *Nature* **227,** 680-685.
41. Becktel, W. J., and Schellman, J. A. (1987) *Biopolymers* **26**, 1859-1877.
42. Yamasaki, T., Kanaya, S., and Oobatake, M. (1995) *Thermochimica Acta* **267**, 379-388.
43. Thornton, J. M. (1981) *J. Mol. Biol.* **151**, 261-287.
44. Anfinsen, C. B., and Scheraga, H. A. (1975) *Adv. Protein Chem.* **29**, 205-300
45. Johnson, R. E., Adams, P. and Rupley, J. A. (1978) *Biochemistry* **17**, 1479-1483.
46. Lin, S. H., Konishi, Y., Denton, M. E. and Scheraga, H. A. (1984) *Biochemistry* **23**, 5504-5512.
47. Pace, C. N., Grimsley, G. R., Thomson, J. A., and Barnett, B. J. (1988) *J. Biol. Chem.* **263**, 11820-11825.
48. Matsumura, M., Becktel, W. J., Levitt, M. and Matthews, B. W. (1989) *Proc. Natl. Acad. Sci. USA* **86,** 6562-6566.
49. Nakamura, H., Oda, Y., Iwai, S., Inoue, H., Ohtsuka, E., Kanaya, S., Kimura, S., Katsuda, C., Katayanagi, K., Morikawa, K., Miyashiro, H. and Ikehara, M.

(1991) *Proc. Natl. Acad. Sci. USA* **88,** 11535-11539.
50. Jiang, Y., Nock, S., Nesper, M., Sprinzl, M. and Sigler, P. B. (1996) *Biochemistry* **35**, 10269-10278
51. Blank, J., Nock, S., Kreutzer, R. and Sprinzl, M. (1996) *Eur. J. Biochem.* **236**, 222-227.
52. Garel, J. -R., and Baldwin, R. L. (1973) *Proc. Natl. Acad. Sci. USA* **76**, 3347-3351
53. Brandts, J. F., Halvorson, H. R., and Brennan, M. (1975) *Biochemistry* **14**, 4953-4963.
54. Kiefhaber, T., Quaas, R., Hahn, U., and Schmid, F. X. (1990) *Biochemistry* **29**, 3053-3061.
55. Goedken, E. R., Raschke, T. M., and Marqusee, S. (1997) *Biochemistry* **36**, 7256-7263.
56. Oda, Y., Yoshida, M., and Kanaya, S. (1993) *J. Biol. Chem.* **268**, 88-92.
57. Haruki, M., Noguchi, E., Nakai, C., Liu, Y. Y., Oobatake, M., Itaya, M. and Kanaya, S. (1994) *Eur. J. Biochem.* **220**, 623-631.
58. Merz, A., Yee, M. C., Szadkowski, H., Pappenberqer, G., Crameri, A., Stemmer, W. P. C., Yanofsky, C., and Kirschner, K. (2000) *Biochemistry* **39**, 880-889.
59. Itaya, M., and Crouch, R. J. (1991) *Mol. Gen. Genet.* **227**, 424-432.
60. Itaya, M., McKelvin, D., Chatterjie, S. K., and Crouch, R. J. (1991) *Mol. Gen. Genet.* **227**, 438-445.
61. Campbell, A. G., and Ray, D. S. (1993) *Proc. Natl. Acad. Sci. U.S.A.* **90**, 9350-9354.
62. Hesslein, D. G. T., and Campbell, A. G. (1997) *Mol. Biochem. Parasitol.* **86**, 121-126.
63. Itaya, M. (1990) *Proc. Natl. Acad. Sci. U.S.A.* **87**, 8587-8591.
64. Zhang, Y-B., Ayalew, S., and Lacks, S. A. (1997) *J. Bacteriol.* **179**, 3828-3836.
65. Haruki, M., Hayashi, K., Kochi, T., Muroya, A., Koga, Y., Morikawa, M., Imanaka, T., and Kanaya, S. (1998) *J. Bacteriol.* **180**, 6207-6214.

66. Stemmer, W. P. C. (1994) *Nature* **370**, 389-390.
67. Dower, W. J., Miller, J. H., and Ragsdale, C. W. (1988) *Nucleic Acids Res.* **16**, 6127-6145.
68. Hirano, N., Haruki, M., Morikawa, M., and Kanaya, S. (1998) *Biochemistry* **37**, 12640-12648.
69. Kanaya, S., Kohara, A., Miura, Y., Sekiguchi, A., Iwai, S., Inoue, H., Ohtsuka, E., and Ikehara, M. (1990). *J. Biol. Chem.* **265**, 4615-4621.
70. Green, N. M., and Melamed, M. D. (1966) *Biochem. J.* **100**, 614-621.
71. Kanaya, S., Oobatake, M., and Liu, Y-Y. (1996) *J. Biol. Chem.* **271**, 32729-32736.
72. Yamasaki, K., Akasako-Furukawa, A., and Kanaya, S. (1998) *J. Mol. Biol.* **277**, 707-722.
73. Hollien, J., and Marqusee, S. (1999) *Proc. Natl. Acad. Sci. U.S.A.* **96**, 13674-13678.
74. Nakai, C., Konishi, A., Komatsu, Y., Inoue, H., Ohtsuka, E. and Kanaya, S. (1994) *FEBS Lett.* **339**, 67-72.
75. Ma, W. P., Hamilton, S. E., Stowell, J. G., Bym, S. R. and Davisson, V. J. (1994) *Bioorg. Med. Chem.* **2**, 169-179.
76. Zuckermann, R. N. and Schultz, P. G. (1988) *J. Am. Chem. Soc.* **110**, 6592-6594.
77. Zuckermann, R. N., Corey, D. R. and Schultz, P. G. (1988) *J. Am. Chem. Soc.* **110**, 1614-1615.
78. Zuckermann, R. N. and Schultz, P. G. (1989) *Proc. Natl. Acad. Sci. U.S.A.* **86**, 1766-1770.
79. Uchiyama, Y., Inoue, H., Ohtsuka, E., Nakai, C., Kanaya, S., Ueno, Y. and Ikehatra, M. (1994) *Bioconjugate Chem.* **5**, 327-332.
80. Kanaya, E., Uchiyama, Y., Ohtsuka, E., Ueno, Y., Ikehara, M. and Kanaya, S. (1994) *FEBS Lett.* **354**, 227-231.
81. Jay, E., Bambara, R., Padmanabham, P. and Wu, R. (1974) *Nucleic Acids Res.* **1**, 331-353.
82. Coffin, J. M. (1996) In Fields, B. N., Knipe, D. M., Howly, P. M., Chanock, R. M., Melnick, J. L., Monath, T. P., Roizeman, B. and Straus, S. E. (eds), *Virology*. 3rd edn. Lippincott-Raven Publishers, New York, NY, pp. 1767-1847.
83. Itakura, K., Rossi, J. J., and Wallace, R. B. (1984) *Annu. Rev. Biochem.* **53**, 323-356.
84. Kanaya, E. and Kanaya, S. (1995) *Eur. J. Biochem.* **231**, 557-562.
85. Iwai, S., Wakasa, M., Ohtsuka, E., Kanaya, S., Kidera, A. and Nakamura, H. (1996) *J. Mol. Biol.* **263**, 699-706.
86. Fedoroff, O. Y., Salazar, M. and Reid, B. R. (1993) *J. Mol. Biol.* **233**, 509-523.
87. Xiong, Y. and Sundaralingam, M. (1998) *Structure* **6**, 1493-1501.
88. Xiong, Y. and Sundaralingam, M. (2000) *Nucleic Acids Res.* **28**, 2171-2176.

List of Publications

1 Stabilization of Ribonuclease HI from *Thermus thermophilus* HB8 by the Spontaneous Formation of an Intramolecular Disulfide Bond
Nobutaka Hirano, Mitsuru Haruki, Masaaki Morikawa and Shigenori Kanaya,
(1998) *Biochemistry* 37, 12640-12648.

2 Enhancement of the Enzymatic Activity of Ribonuclease HI from *Thermus thermophilus* HB8 with a Suppressor Mutation Method
Nobutaka Hirano, Mitsuru Haruki, Masaaki Morikawa and Shigenori Kanaya,
(2000) *Biochemistry* 39, 13285-13294.

3 Efficient cleavage of RNA at high temperatures by a thermostable DNA-linked ribonuclease H
Mitsuru Haruki, Tomoko Nogawa, Nobutaka Hirano, Hyongi Chon, Yasuo Tsunaka, Masaaki Morikawa, and Shigenori Kanaya
Protein engineering, in press.

Acknowledgments

I wish to express my sincere thanks to Professor Dr. Shigenori Kanaya for his guidance, helpful discussion, suggestions, encouragement, and continuous support throughout the course of this study.

I am deeply grateful to Associate Professor Dr. Masaaki Morikawa for his helpful comments and suggestions throughout the course of this study.

I wish to express grateful to Assistant Professor Dr. Mitsuru Haruki for his helpful discussion, suggestions, encouragement, and valuable advice in experimental procedures throughout the course of this study.

I would like to sincerely acknowledge Professor Dr. Shunichi Fukuzumi and Professor Dr. Itaru Urabe for careful reading this thesis and valuable comments.

I would like to thank to Dr. Motohisa Oobatake, Dr. Mitsuhiro Itaya, Dr. Eiko Kanaya and Dr. Robert J. Crouch for their advice and supports in experimental procedures.

I also would like to thank to my co-workers, Ms. Tomoko Nogawa, Mr. Hyongi Chon, and Mr. Yasuo Tsunaka, for their helpful discussion and technical contribution. A lot of thanks are due to members of RNase H group of Kanaya's laboratory, Mr. Naoto Ohtani, Mr. Ayumu Muroya, Mr. Takayuki Kochi, and Mr. Rikita Nakano, for their helpful discussion and suggestions. Special thanks are due to all the present members of Kanaya's laboratory, in particular Mr. Yuichi Koga, as well as all the past members of Kanaya's laboratory, in particular Mr. Tomoyoshi Koyanagi, Mr. Kiwamu Takemoto, and Mr. Tomoki Matsuda, for their friendship and encouragement. Special thanks are also due to Mrs. Reiko Matsumoto for her kindness.

Finally, my particular gratitude goes to my family for their hearty encouragement and supports.

March, 2001

Nobutaka Hirano